



AMERICAN METEOROLOGICAL SOCIETY

Bulletin of the American Meteorological Society

EARLY ONLINE RELEASE

This is a preliminary PDF of the author-produced manuscript that has been peer-reviewed and accepted for publication. Since it is being posted so soon after acceptance, it has not yet been copyedited, formatted, or processed by AMS Publications. This preliminary version of the manuscript may be downloaded, distributed, and cited, but please be aware that there will be visual differences and possibly some content differences between this version and the final published version.

The DOI for this manuscript is doi: [10.1175/BAMS-D-11-00136.1](https://doi.org/10.1175/BAMS-D-11-00136.1)

The final published version of this manuscript will replace the preliminary version at the above DOI once it is available.



1
2 **The CIRCE simulations: a new set of regional**
3 **climate change projections performed with a**
4 **realistic representation of the Mediterranean Sea**

5
6
7 Gualdi S.^{1,2}, S. Somot³, L. Li⁴, V. Artale⁵, M. Adani², A. Bellucci¹, A. Braun³, S. Calmanti⁵,
8 A. Carillo⁵, A. Dell'Aquila⁵, M. Déqué³, C. Dubois³, A. Elizalde⁶, A. Harzallah⁷, D. Jacob⁶,
9 B. L'Hévéder⁴, W. May⁸, P. Odno², P. Ruti⁵, A. Sanna¹, G. Samino⁵, E. Scoccimarro², F.
10 Sevaut³ and A. Navarra^{1,2}

11
12
13 1 Centro Euro-Mediterraneo per i Cambiamenti Climatici, CMCC, Bologna, Italy

14 2 Istituto Nazionale di Geofisica e Vulcanologia, INGV, Bologna, Italy

15 3 Météo France, CNRM-GAME, Toulouse, France

16 4 Laboratoire de Météorologie Dynamique, CNRS-LMD, Paris, France

17 5 Italian National Agency for New Technologies, Energy and Sustainable Economic Development, ENEA, Rome, Italy

18 6 Max-Planck Institute for Meteorology, MPI, Hamburg, Germany

19 7 National Institute of Marine Sciences and Technologies, INSTM, Salammbou, Tunisia

20 8 Danish Meteorological Institute, DMI, Copenhagen, Denmark

21
22
23 Corresponding author: Silvio Gualdi, email: silvio.gualdi@cmcc.it

24
25
26
27
28
29
30 Submitted to BAMS (May, 2011)

31 Revised Version (January 2012)

32 Second Revision (May 2012)

33
34
35
36 **Capsule:** Climate change projections for the Mediterranean region performed
37 improving the representation of the Mediterranean Sea into the climate system

38
39
40

Abstract

41
42 In this article we describe an innovative multi-model system developed within the CIRCE
43 EU-FP6 Project and used to produce simulations of the Mediterranean Sea regional climate.
44 The models include high-resolution Mediterranean Sea components, which allow to assess the
45 role of the basin, and in particular of the air-sea feedbacks in the climate of the region.
46 The models have been integrated from 1951 to 2050, using observed radiative forcings during
47 the first half of the simulation period and the IPCC SRES A1B scenario during the second
48 half.
49 The projections show a substantial warming (about 1.5°-2°C) and a significant decrease of
50 precipitation (about 5%) in the region for the scenario period. However, locally the changes
51 might be even larger. In the same period, the projected surface net heat loss decreases, leading
52 to a weaker cooling of the Mediterranean Sea by the atmosphere, whereas the water budget
53 appears to increase, leading the basin to loose more water through its surface than in the past.
54 These results are overall consistent with the findings of previous scenario simulations, such as
55 PRUDENCE, ENSEMBLES and CMIP3. The agreement suggests that these findings are
56 robust to substantial changes in the configuration of the models used to make the simulations.
57 Finally, the models produce a 2021-2050 mean steric sea-level rise that ranges between +7 cm
58 and +12 cm, with respect to the period of reference.

59

60 **1. The problem of the Mediterranean Region Climate Simulations**

61 The climate of the Mediterranean region, defined here as the area including the Mediterranean
62 Sea and the surrounding areas, is determined by the interaction between mid-latitude and sub-
63 tropical circulation regimes with the complex morphology (mountain chains and land-sea
64 contrasts) that characterizes this part of the Earth. The region has been identified as one of the
65 main climate change hot-spots, i.e. one of the most responsive areas to climate change (Giorgi
66 2006). The area is populated by over 500 million people, distributed in about 30 countries in
67 Africa, Asia and Europe. Therefore, understanding climate variability here has also important
68 social implications.

69 In the recent past, a number of scientific initiatives and projects have been undertaken to
70 assess the possible changes that anthropogenic global warming might induce in the climate of
71 the European continent and of the Mediterranean region. Specifically, scenario simulations
72 aimed at quantifying the possible future climate change in the European and Mediterranean
73 region have been designed and performed in the framework of EU Projects such as
74 PRUDENCE (Christensen and Christensen 2007) and ENSEMBLES (Christensen et al.
75 2009). At the same time, coordinated studies have been performed to investigate and to assess
76 the climate change signal in the Mediterranean region projected by both regional and global
77 models (Giorgi and Lionello 2008). Marcos and Tsimplis (2008), for example, used the
78 CMIP3 data (Meehl et al. 2007) to assess the uncertainty range of the response of the
79 Mediterranean Sea temperature, salinity and sea level change during the 21st century.
80 According to their findings, the CMIP3 general circulation models (GCMs) reveal many
81 difficulties in simulating a realistic Mediterranean Sea in present climate because of their low
82 spatial resolution. Therefore, also the climate change signal produced by these models in the
83 Mediterranean region should be considered with some caution. Using the same dataset,
84 Mariotti et al. (2008) quantified the change in the regional water budget components. A

85 similar analysis has been done by Sanchez-Gomez et al. (2009), using the outputs of the
86 ENSEMBLES atmosphere-only regional climate models (RCMs), with 25 km resolution over
87 the Mediterranean Sea, for the A1B scenario. Their results show that both global and regional
88 models produce climate scenarios characterized by a significant drying of the Mediterranean
89 region, mainly after year 2050 of the emission scenarios.

90 Concerning the impact of the climate change on the Mediterranean Sea, so far very few
91 studies have been specifically devoted to this basin. Furthermore, all of these studies were
92 conducted with just one climate model, leaving largely unresolved the fundamental issue of
93 the uncertainty associated with the choice of the model. A pioneering work was done by
94 Thorpe and Bigg (2000) simulating a transient $2\times\text{CO}_2$ scenario with a $1/4^\circ$ -resolution ocean
95 model forced by the air-sea fluxes of a low-resolution IPCC model ($2.5^\circ\times 3.5^\circ$). Later, Somot
96 et al. (2006) performed a similar study using a higher-resolution ocean model ($1/8^\circ$) forced by
97 fluxes coming from a dynamical downscaling (50 km) of an A2 IPCC run. Both studies show
98 an increase of the sea surface temperature (SST) and sea surface salinity (SSS), leading to a
99 strong weakening of the Mediterranean thermohaline circulation (MTHC) and a change in the
100 characteristics of the Mediterranean waters out-flowing at the Gibraltar Strait. The latter study
101 took into account the climate change impact coming from all the various forcings of the
102 Mediterranean Sea (air-sea fluxes, Atlantic characteristics, river runoff and Black Sea impact)
103 concluding that all of them could be important contributors to the possible evolution of the
104 sea characteristics.

105 Most of the above mentioned works are based either on global low-resolution ocean-
106 atmosphere coupled climate models (AOGCMs) or stand alone (atmosphere-only or ocean-
107 only) high-resolution regional models. Each of two approaches presents advantages and
108 weaknesses. An important shortcoming common to the global coupled and regional
109 atmosphere only models is their limited capability to include into the climate change

110 projections for this region a realistic representation of the processes associated with the
111 presence of the Mediterranean Sea. The global AOGCMs used so far have horizontal
112 resolutions generally not sufficient to represent the complexity of the geomorphology of the
113 region. In Figure 1, panels a and b show the Mediterranean Sea and the surrounding mountain
114 chains (Atlas, Alps and Caucasus Mountains) as they are represented in a global model with a
115 horizontal resolution of about 300 km in the atmosphere and about 100 km in the ocean. This
116 is the order of resolution employed, for example, in several models used to perform the
117 CMIP3 simulations (Meehl et al, 2007). It appears evident that a number of important
118 features, such as, for example, the complex topography, the islands, the straits and the
119 coastlines of the Mediterranean Sea itself are only barely resolved. Therefore, these models
120 reproduce the small-scale physical processes that characterize the climate behaviour of the
121 region very poorly.

122 On the other hand, the atmosphere-only regional models used so far to downscale the
123 global simulations, such as those, for example, employed in the PRUDENCE or
124 ENSEMBLES EU-Projects, are usually implemented with horizontal resolutions ranging
125 from 50 km to 20 km, which according to Gibelin and Déqué (2010) and Gao et al. (2006)
126 should be sufficient to simulate a realistic circulation over the Mediterranean Sea and the
127 European continent. These models, however, are forced with prescribed lower boundary
128 conditions (SSTs) and thus they do not take into account any air-sea feedbacks. The lack of
129 these feedbacks reduces the consistency between SST, air-sea fluxes and vertical structure of
130 the atmosphere (air-sea coupling), diminishing the confidence in the modelling results over
131 the Euro-Mediterranean area (Somot et al. 2008). Furthermore, the Mediterranean SST used
132 to force the models over the basin are produced with low-resolution AOGCMs, which are
133 inadequate to reproduce the small scale features that distinguish the behaviour of this sea

134 (e.g., Marcos and Tsimplis 2008). Similar arguments hold for regional ocean-only model
135 simulations, where air-sea feedbacks are not fully considered.

136 The deficiencies in including a realistic modelling of the Mediterranean Sea into the
137 climate system might have considerable consequences on the quality and reliability of the
138 climate change projections that state-of-the-art models (both global and regional) provide for
139 the Mediterranean area and the European continent. A first attempt to remedy these
140 deficiencies has been made by Somot et al. (2008) who developed an atmosphere-ocean
141 regional climate model (AORCM), coupling a variable resolution version of a global
142 atmospheric model with a high-resolution oceanic model of the Mediterranean Sea (see
143 Somot et al. 2008 for additional details). According to their results, the coupled model
144 appears to be in good agreement with the observations over the Mediterranean region for the
145 reference period 1961-1990. Moreover, it appears to perform as well as or even better than
146 most of the PRUDENCE state-of-the-art uncoupled regional models forced with observed
147 SSTs in the Mediterranean basin. Importantly, Somot et al. (2008) found also substantial
148 differences between the regional coupled and uncoupled climate change projections, which
149 can be ascribed to the inclusion of the Mediterranean Sea model.

150 In the framework of the CIRCE (Climate Change and Impact Research: the Mediterranean
151 Environment) EU project, a set of coupled models has been developed with the aim of
152 producing climate change projections for the Mediterranean region. Following Somot et al.
153 (2008), all of the models include a high-resolution numerical model of the Mediterranean Sea
154 and thus they can simulate the small-scale features of the basin. They have been integrated to
155 produce multi-model ensemble simulations of the present climate and future change
156 projections. The multi-model ensemble approach adopted in CIRCE is one of the techniques
157 most frequently used to assess the uncertainties that can arise from different types of model
158 errors (Deque et al. 2007). This approach provides an estimate of the uncertainty due to

159 structural variations among a range of models by combining them, with the main assumption
160 of a quasi-independent development of the considered models and excluding any systematic
161 analysis of individual sources of errors. In general, the multi-model ensemble experiments are
162 not specifically designed to provide formal error estimates. They are in essence “ensembles of
163 opportunity” and the ensemble spread can be seen as a tool to characterize the model
164 uncertainty. The CIRCE experiments, thus, will allow the quantification of the Mediterranean
165 Sea response to climate change, providing also an estimate of the uncertainty associated with
166 the choice of models, though the relatively small size of the multi-model ensemble (five
167 members) will not allow a comprehensive and statistically robust uncertainty assessment.

168 In the following we will discuss the basic characteristics of the CIRCE models, their
169 ability to simulate the major features of the observed climate in the Mediterranean region and
170 how these features might be possibly affected by the global warming in the next few decades.

171 **2. The CIRCE models**

172 The major novelty featured by the CIRCE models compared with the climate models
173 commonly used to produce scenario simulations is the inclusion of a realistic representation
174 of the Mediterranean Sea into the climate system. To achieve the aim, the CIRCE models
175 include high-resolution atmospheric components fully coupled with high-resolution models of
176 the Mediterranean Sea able to resolve those small-scale features that characterize the
177 physiography of the basin, as it is shown in Figure 1 (panels c and d).

178 Figure 2 provides a schematic representation of the implementation of the CIRCE models.
179 All of the models have a relatively high-resolution atmospheric component over the
180 Mediterranean region (ranging from 80 to 25 km) that can be either stretched/global or
181 limited-area over this region. These atmospheric components are coupled with a high-
182 resolution model of the Mediterranean Sea, exchanging local air-sea fluxes. When the

183 atmospheric model is global (Figure 2, left panel), the rest of the global ocean is represented
184 by a global low-resolution ocean model coupled with the Mediterranean Sea in the vicinity of
185 the Strait of Gibraltar. When the atmospheric component is regional (Figure 2, right panel),
186 the lateral boundary conditions for both the limited-area atmosphere and the Mediterranean
187 Sea models are provided by global simulations.

188 Table 1 summarizes the main characteristics of the CIRCE models along with references
189 where more detailed descriptions of the models' features and in depth discussions of the
190 technical aspects are made. Here, for the sake of brevity, we provide only a general overview
191 of the modelling strategy, in order to illustrate the basic characteristics of the CIRCE
192 approach. In three cases (CMCC, CNRM and LMD), the Mediterranean Sea component is
193 coupled with a global atmosphere and, in a region near Gibraltar, with a global ocean. In these
194 models, every atmosphere-ocean coupling time step (~3 hours for CMCC and daily for
195 CNRM and LMD), heat (radiative and turbulent fluxes), mass (evaporation, precipitation and
196 runoff) and momentum fluxes are provided to the ocean models (both global and
197 Mediterranean) by the atmospheric model. At the same time, the atmosphere receives the
198 global SST and the sea-ice distribution values from the global ocean and the SST in the
199 Mediterranean Sea from the Mediterranean model. The communications between the oceanic
200 and atmospheric components are carried out with the coupler OASIS3 (Valcke 2006).

201 The global and Mediterranean ocean components, on the other hand, exchange the
202 coupling fields in a so-called "Atlantic box" (a relatively large area located to the west of
203 Gibraltar) via oceanic open boundaries, where the exchanged quantities (profiles of
204 temperature, salinity, zonal and meridional velocity and sea surface elevation) are suitably
205 interpolated. The coupling occurs every 8 hours in the CMCC model and on daily basis in the
206 CNRM and LMD models. The Atlantic characteristics in these modes evolved interactively in

207 the global refined models as the Mediterranean Sea component is fully coupled to the global
208 ocean.

209 The climate simulations produced with these models (CMCC, CNRM and LMD), thus,
210 account for the regional-scale processes that characterize the Mediterranean basin and
211 provide, for the first time, the possibility to accurately assess the role and feedbacks of the
212 Mediterranean Sea in the global climate system.

213 In the remaining two models (ENEA and MPI), the Mediterranean Sea is coupled with a
214 high-resolution atmospheric limited area component. The coupling, done through OASIS3, is
215 similar to the one implemented for the global models: heat, moisture and momentum fluxes
216 are passed from the limited area atmosphere to the Mediterranean Sea component, and the
217 latter returns SSTs to the atmospheric model with a coupling frequency of 6 hours. In this
218 case, however, the coupled simulations are conducted prescribing lateral boundary conditions
219 both for the atmosphere and for the ocean (in the Atlantic box). Specifically, the lateral
220 boundary conditions for the MPI model are obtained from the CMCC model simulation
221 (Scoccimarro et al, 2011), whereas the ENEA model uses data from the ECHAM5/MPI-OM
222 CMIP3 simulations (Giorgetta et al. 2006). Therefore, in contrast with the CMCC, CNRM
223 and LMD models, where the Mediterranean component is fully coupled to the global ones, in
224 these regional coupled models (ENEA and MPI) the Mediterranean Sea does not provide
225 feedbacks to the global climate system. However, the coupling between the high-resolution
226 atmospheric and Mediterranean Sea components are expected to improve the consistency
227 between SSTs, air-sea fluxes and vertical structure of the atmosphere (air-sea coupling) with
228 respect to the coarse resolution global driver (Dell'Aquila et al. 2012) and thus to better
229 simulate ocean-atmosphere feedbacks thereby providing more confidence in present and
230 future climate changes over the Mediterranean region (Somot et al. 2008).

231 Rivers are interactively coupled to the atmosphere and ocean models for ENEA, CMCC
232 and MPI and are, thus, impacted by the climate change signals. In the CNRM and LMD
233 models, on the other hand, river discharges are kept constant at the observed monthly
234 climatological values, as they are not provided of a suitable river routing scheme. In the
235 scenario simulations, the climatological values of river discharge used in these two models,
236 thus, are not consistent with the possible changes in land precipitation. A discussion of the
237 implications of this choice has been done in Dubois et al. (2012). However, the river
238 discharge is the smaller component of the water budget in the Mediterranean Sea and the error
239 we make using climatological values is smaller than other approximations we make. For
240 example, in reality in many Mediterranean rivers the actual discharge is strongly modulated
241 by human activities, such as water demand for agriculture purposes (e.g., Lopez-Moreno,
242 2008). These land use changes are only marginally considered in the CIRCE models.

243 The Black Sea contribution to Mediterranean water budget (B) is treated differently in the
244 different models. In the MPI case, where the Black Sea is explicitly represented, B is the net
245 water transport computed at the Dardanelles Strait. In the CMCC and in the ENEA models,
246 the B contribution is defined as the residual of the E-P-R (Evaporation-Precipitation-Runoff)
247 budget for this basin in the atmospheric model. Then, following Somot et al. (2006), the
248 budget is used as a freshwater input in the Aegean Sea. However, in the ENEA case, the
249 computed values have been rescaled using monthly coefficients derived from a previous run
250 forced by reanalysis in order to match observations (Dell'Aquila et al. 2011). The LMD and
251 CNRM models, on the other hand, used monthly climatological values (Beuvier et al. 2010).

252 The water and heat budget of the Mediterranean Sea are controlled also by the water
253 exchanges with the Atlantic Ocean, through the Strait of Gibraltar. Such exchanges are highly
254 variable, with strong fluctuations ranging from semidiurnal to seasonal and interannual time-
255 scales. Provision of a realistic reproduction of the physical processes that regulate the water

256 exchange between Mediterranean Sea and Atlantic Ocean at the Strait of Gibraltar is not
257 straightforward. Recent works indicate that in order to make realistic simulations of the water
258 exchanges at Gibraltar, a model should have very high resolution (both in horizontal, about
259 500 m, and in vertical, about 10 m, directions), it should include explicit tidal forcing, and it
260 should be implemented with physical parameterizations taking into account diapycnal mixing
261 and entrainment (e.g. Sannino et al 2009b and references therein). A model that has these
262 characteristics would be able to properly reproduce the small-scale mechanisms that govern
263 the water flow through Gibraltar and its hydraulic criticality (Sannino et al. 2009). However,
264 the explicit representation of such small-scale processes in numerical models of the
265 Mediterranean Sea designed for climate studies, and therefore running over several decades,
266 is extremely demanding on computing resources and, at the present, beyond the available
267 resources at many research centres. Thus, also in the CIRCE models the Strait of Gibraltar is
268 modelled using only few grid points and vertical levels, and, in some cases, using relatively
269 simple parameterizations for entrainment and mixing processes. Specifically, for the physical
270 parameterization for entrainment and mixing processes applied at the strait, CMCC uses an
271 up-stream advection scheme for active tracers, whilst in the rest of the basin a MUSCL
272 (Monotonic Upwind Scheme for Conservation Laws, Van Leer 1979) scheme is adopted. The
273 vertical diffusivity in this area, between 30 and 150 m depth, is increased in order to
274 parameterise unresolved processes induced by vertical mixing. In the same geographical area
275 the bottom friction drag coefficient is linear and five times larger than in the other parts of the
276 model. ENEA increases the vertical diffusion 10 times with respect to the rest of the model in
277 the Strait area, and replaces the horizontal bi-Laplacian viscosity with a Laplacian viscosity.
278 MPI, CNRM, and LMD do not apply any specific parameterization (Dubois et al. 2012 and
279 Elizalde et al. 2010).

280 **The simulations**

281 The models described above have been used to make climate simulations of the second part of
282 the 20th Century (1951-2000) and the first part of the 21st Century (2001-2050). During the
283 20th Century period of the simulations, the distribution and concentration of the atmospheric
284 greenhouse gases (GHGs) and aerosol (anthropogenic sulfate only) have been specified from
285 observations, as it has been done for the CMIP3 20th Century integrations (hereafter referred
286 to as 20C3M, Meehl et al. 2007). During the 21st Century period, on the other hand, the
287 GHGs and anthropogenic aerosol have been specified according to the A1B IPCC-SRES
288 scenario (Nakicenovic et al. 2000).

289 The model simulations have been initialized with the Levitus (Levitus 1982) or MedAtlas-
290 II (MEDAR-Group 2022) climatology as initial conditions for the ocean and either
291 atmospheric re-analyses or AMIP-type simulations (i.e. simulations where the atmospheric-
292 only model has been integrated using observed SST as boundary conditions) for the
293 atmosphere. A spin-up of several decades of the coupled system has then been performed by
294 integrating the model with the 1950's permanent conditions (radiative forcing). For example,
295 in the case of the CMCC model, the global coupled system (global atmosphere and global
296 ocean) has been integrated for about 200 years and then the Mediterranean Sea model has
297 been added to the system and another 50-year spin-up integration has been done. A similar
298 spin-up procedure has been used with the other models (for additional details, please see the
299 references reported in Table 1) and, in most of the cases it has allowed the models to reach a
300 reasonably stable state (i.e. no significant long-term temperature drift was found for the upper
301 ocean). Only in one case, the LMD model, there is some evidence that, despite the spin-up,
302 the bottom water of the Mediterranean Sea (deeper than 1000 m) is still affected by a cooling
303 trend at the beginning of the CIRCE integration that will affect the behaviour of the whole
304 water column for the earlier decades of the simulation, as we will see in the computation of
305 the steric effect in Section 3.

306 Once the model spin-up has been completed, the GHGs and aerosols have been changed
307 according to the 20C3M radiative forcing up to year 2000 and afterwards, from year 2001 to
308 2050, following the A1B scenario. As shown in Table 1, the ENEA and MPI models have
309 been integrated using boundary conditions from the 20C3M and A1B simulations performed
310 with ECHAM5MPI-OM (Giorgetta et al. 2006) and with the CMCC CIRCE simulation
311 respectively.

312 More detailed descriptions and in depth discussions of the models' features and how the
313 simulations have been conducted can be found in Dubois et al. (2012), Gualdi et al. (2012)
314 and in the documentation papers and reports listed in Table 1.

315 **3. Some results from the CIRCE projections**

316 Here we illustrate some basic findings obtained from the CIRCE simulations, with the aim
317 of providing a quick overview and summary of the results of the CIRCE models and their
318 potential, especially for climate change impact studies in the Mediterranean region. A more
319 extended and detailed discussion of the results obtained from the CIRCE models can be found
320 in Artale et al. (2010), Gualdi et al. (2012), Dubois et al. (2012), Elizalde (2011) and
321 Dell'Aquila et al. (2011).

322 Overall, the CIRCE models appear to reproduce reasonably well many of the observed
323 features related to the orographic forcing. Compared to the CMIP3 models, the simulation, for
324 example, of the seasonal mean precipitation over the north-west of the Iberian Peninsula,
325 Alpine region, western coast of the Balkans and south-west Anatolian Peninsula seems to be
326 locally improved. Despite these local improvements, the overall model systematic errors over
327 the region remain substantial, both in terms of T2m and precipitation (Gualdi et al. 2012).
328 During both winter (DJF) and summer (JJA), the models are generally colder than
329 observations by about 2°C over most of the Mediterranean area.

330 Over land, larger errors, though confined to very small areas, are found locally in the
331 northern foothills of the Alps (about -6°C), whereas a warm bias (about $+4^{\circ}\text{C}$) covers the
332 south-eastern part of the Alpine region. The models tend also to overestimate the precipitation
333 over central Europe in both seasons, whereas rainfall tends to be underestimated in the Alpine
334 region, Middle East and, in JJA, in the area of the Black Sea. A more detailed description of
335 the CIRCE models' errors can be found in Gualdi et al. (2012).

336 Over the sea, the SST error appears to be rather uniform across the basin and can be
337 explained by either too cold air-sea fluxes during the spin-up integration coming from the
338 atmospheric model or by the advection of too cold waters through the Gibraltar Strait (Dubois
339 et al. 2012, Dell'Aquila et al. 2011).

340 Despite the systematic error, however, most of the CIRCE models reproduce reasonably
341 realistic patterns of near surface temperature and precipitation and a realistic structure of the
342 Mediterranean SST, especially, of the observed SST gradients.

343 In order to provide an overall estimation of the capability of the CIRCE models in
344 reproducing the main features of the observed Mediterranean climate, we computed the
345 Taylor diagrams (Taylor 2001) of the T2m, precipitation and SST seasonal means (Figure 3).
346 In this application, the simulated means are compared to the observed ones, with the spatial
347 standard deviation and its associated root mean square difference (RMSD) plotted in relation
348 to the pattern correlation. Specifically, Figure 3 shows the Taylor diagrams of the simulated
349 Mediterranean SST averaged over the basin, and T2m and precipitation over land averaged
350 over the Mediterranean area (28° - 48°N , 9.5°W - 38.5°E). The observations used in the analysis
351 are T2m and precipitation obtained for the period 1971-2000 from the gridded observations
352 (CRU-TS.3, Mitchell and Jones, 2005) and the high-resolution SST re-analysis for the
353 Mediterranean Sea (Adani et al. 2011) for the period 1985-2000. A similar analysis has been
354 done using the Mediterranean SST from the HadISST data set (Rayner et al. 2003) for the

355 period 1971-2000 and the results obtained are fully consistent with those shown in Figure 3
356 panels a and b.

357 Furthermore, to provide also a comparison between the CIRCE and the CMIP3 models'
358 performance, we included in the diagrams the results obtained from a set of CMIP3
359 simulations. Importantly, the purpose of this work is neither to provide an exhaustive
360 assessment of the differences between the CIRCE and the CMIP3 models nor to study all of
361 the simulations available in the CMIP3 database. Thus, the set of CMIP3 models and
362 simulations that we consider here is not comprehensive. With the ten CMIP3 models
363 presented in Table 2 and considered in the analysis, we expect to have a representative sample
364 of the performance of state-of-the-art coupled models in simulating the Mediterranean region
365 climate and its possible projected changes. More information about the CMIP3 models can be
366 found on the CMIP3 website at PCMDI: [http://www.pcmdi.llnl.gov/ipcc/model](http://www.pcmdi.llnl.gov/ipcc/model_documentation/ipcc_model_documentation.php)
367 [documentation/ipcc_model_documentation.php](http://www.pcmdi.llnl.gov/ipcc/model_documentation/ipcc_model_documentation.php).

368 Overall, the majority of CMIP3 models (indicated with a + in the pictures of Figure 3)
369 underestimate the spatial standard deviation. In several cases, the CIRCE models (coloured
370 dots) appear to be closer to observations (black dot), though the spatial standard deviation of
371 precipitation in DJF and T2m and SST in JJA tend to be slightly overestimated. Moreover, the
372 majority of the CIRCE models have larger pattern correlations and smaller RMSDs than the
373 CMIP3 ones. The Taylor diagrams of the multi-model ensemble means (indicated with \diamond for
374 the CMIP3 case and with \square for the CIRCE case) give further evidence of the slight
375 improvement of the CIRCE Mediterranean SST, land T2m and land precipitation compared to
376 the CMIP3 models.

377 Noteworthy, both in the CIRCE and CMIP3 ensembles, the multi-model means appear to
378 be in better agreement with observations than any of the individual models. This result is
379 consistent with previous findings (e.g., Glecker et al. 2007), where much wider ranges of

380 physical variables were considered and analyzed. Pincus et al. (2008) suggested that the
381 improvement associated with the multi-model means is generally due to both the spatial
382 smoothing and the model systematic errors compensation performed by the multi-model
383 averaging.

384 Finally, also the amplitude of the multiannual (interannual and decadal) variability (not
385 shown) appears to be reasonably well captured by the CIRCE models both in terms of spatial
386 distribution and amplitude, with maximum values of about 1°C.

387 **Near-surface temperature and precipitation**

388 The evolution of the simulated near-surface temperature averaged over the Mediterranean
389 land during the recent past is in substantial agreement with the observations, showing that the
390 region surrounding the Mediterranean Sea has been warming during most of the 20th Century.
391 During the period 1951-2000 the ensemble mean warming trend is about $0.1 \pm 0.04^\circ\text{C}/\text{decade}$
392 (statistically significant at the 95% level, according to Mann-Kendall trend test). The increase
393 of the low-level temperature is found to have a remarkable spatial and seasonal modulation.
394 During northern summer, the trend over western and central Europe appears to be larger than
395 in the winter season. The largest trend (up to $0.2^\circ\text{C}/\text{decade}$) is found in JJA over the Iberian
396 Peninsula and western part of North Africa. Importantly, the simulated trends found for the
397 second half of the 20th Century are consistent with the results obtained from the observations
398 for the instrumental period (1951-2005, Ulbrich et al. 2012).

399 A more in depth discussion of the trends of T2m and precipitation observed in the
400 Mediterranean region and a comparison between the observed values and the CIRCE
401 simulations can be found in Ulbrich et al. (2012) and Gualdi et al. (2012).

402 The CIRCE projections for the 21st Century suggest that remarkable changes in the
403 climate of the Mediterranean region might occur already in the next few decades of the
404 scenario, showing a rather steadily increase of the near-surface temperature that leads the

405 Mediterranean lands (i.e., the land comprised within the area 28°-47°N, 10°W-40°E) to be
406 substantially warmer at the end of the integration period with respect to the 1961-1990 mean.
407 The increment of the mean temperature is particularly pronounced in southern Europe and
408 Northern Africa in summer (JJA) and over the Alps, where during both winter and summer
409 season the projected 2021-2050 mean warming appears to be as large as 2°C.

410 The evolution of the simulated Mediterranean SST (Figure 4) shows no clearly discernable
411 trends during the early period of the integration (1951-1980), then a positive trend appears to
412 emerge, starting from the second half of the 1980s. The mean SST warming found for the
413 period 2021-2050 compared to the reference period 1961-1990 ranges between +0.8 °C and
414 1.8°C.

415 The regional characteristics of the projected changes in different sub-regions of the
416 Mediterranean area are shown in Figure 5, where the changes in mean T2m (right panels) and
417 precipitation (left panels) are plotted. In particular, the pictures show the changes over seven
418 sub-regions obtained as the differences between the mean for the period 2021-2050 and the
419 reference period 1961-1990. The sub-regions are defined according to Giorgi and Lionello
420 (2008) as: whole Mediterranean (Med) 28°-48°N, 9.5°W-38.5°E; Northern Mediterranean
421 (NMed) 41°-48°N, 9.5°W-38.5°E; Southern Mediterranean (SMed) 28°-41°N, 9.5°W-38.5°E;
422 Western Mediterranean (WMed) 28°-44°N, 9.5°W-10.5°E; Central Mediterranean (CMed)
423 28°-46°N, 10.5°E-20.5°E; Eastern Mediterranean (EMed) 28°-44°N, 20.5°W-38.5°E; Alpine
424 region (ALPS) 44°-48°N, 5.5°E-15.5°E).

425 Figure 5 offers also the opportunity to compare the CIRCE projected change with the
426 signal obtained from the considered CMIP3 models. Furthermore, it provides a first
427 assessment of the differences (spread) between the results obtained from the different CIRCE
428 models (+ symbols), which are an important component of the uncertainties that affect the
429 CIRCE projections.

430 The results shown in Figure 5 left panels indicate that the projected warming appears to be
431 relatively uniform across the considered sub-regions during JJA. In this season, all of the
432 areas appear to be affected by a mean increase of T2m which ranges between about 1.75°C
433 and 2°C in the CIRCE models and between 1.5 and 1.75°C in the CMIP3 ones. During winter
434 (DJF, Figure 5, upper left panel), there are more pronounced differences between the
435 responses of the sub-regions to the radiative forcing. The Alpine region, for example, appears
436 to be more sensitive, showing a larger warming, particularly pronounced in the CIRCE
437 projections. Also the spread of the results obtained from the different CIRCE models exhibits
438 some substantial spatial and seasonal dependency. The difference between the model
439 projections in the Northern Mediterranean (NMed) and in the Alps is significantly larger than
440 the model spread found for the Southern or Eastern Mediterranean (SMed or EMed),
441 especially during northern winter. Importantly, during both seasons, there is a remarkable
442 agreement between the CIRCE and CMIP3 T2m projected changes, at least in terms of their
443 multi-model ensemble means.

444 The changes in precipitation (Figure 5, right panes) show a clear tendency towards dryer
445 conditions for the whole Mediterranean area, which is visible in both seasons, but more
446 pronounced during summer. Overall, the change in precipitation between the 2021-2050
447 seasonal means and the seasonal means for the reference period is of about -5%. The model
448 results show reduced rainfall over most of the sub-regions, even if the uncertainty due to the
449 CIRCE model spread appears to be higher than for the T2m case. During summer (right lower
450 panel), the reduction of precipitation appears to characterize all of the sub-regions, whereas in
451 winter (upper left panel) the precipitation response appears to be different in the northern part
452 of the Mediterranean area compared to the rest of the domain. Here, no substantial change
453 (NMed) or even some rainfall increase (ALPS) is found, in agreement with the findings of
454 Giorgi and Lionello (2008). Finally, also for the projected precipitation changes the results

455 obtained from the CIRCE models appear to be remarkably consistent with the CMIP3
456 simulations, especially for the DJF season.

457 The tendency towards a warmer and dryer climate for the Mediterranean region in the next
458 decades is consistent with the change in surface circulation suggested by the change found in
459 the projected mean sea-level pressure (MSLP, not shown). In DJF, a large area of increased
460 MSLP covers the entire Mediterranean region, which, thus, appears to be characterized by
461 increased anti-cyclonic circulation and enhanced stability. Furthermore, the increased anti-
462 cyclonic circulation associated with the enhanced Mediterranean surface pressure is, in turn,
463 associated with a northward shift of the Atlantic storm track. Both the increased stability and
464 the northward displacement of the storm track have the effect of reducing the cyclonic activity
465 in the Mediterranean basin, which is consistent with the decreased winter precipitation found
466 in the projections. These results are in agreement with previous results based on the CMIP3
467 climate projections (Giorgi and Lionello 2008), with the trends in MSLP found in the
468 observations during the instrumental period (Ulbrich et al. 2011) and with the PRUDENCE
469 climate change projections (Christensen and Christensen 2007). The consensus that we see
470 between the CIRCE projections and the results obtained from previous investigations leads to
471 think that these findings are considerably robust to substantial changes in the configuration of
472 the climate models used to produce the scenario simulations.

473 **Changes in the Mediterranean Water Budget**

474 The trends in temperature and precipitation found in the CIRCE projections are also
475 associated with a more vast change, involving the Mediterranean basin and its hydrologic
476 cycle in particular. Over the land surrounding the Mediterranean basin, projected evaporation
477 shows very little change in winter and a clear tendency to decrease in summer, whereas over
478 the sea it appears to increase both in winter and in summer. Noteworthy, these findings are
479 fully consistent with Held and Soden (2006). The projected value of the budget evaporation-

480 precipitation (E-P) shows a marked positive trend, both over the sea and over the surrounding
481 lands, due to the combined effect of increased evaporation and reduced precipitation, in
482 agreement with results of Mariotti et al. (2008) and Sanchez-Gomez et al. (2009) obtained
483 using the CMIP3 and the ENSEMBLES simulations respectively.

484 The analysis of the simulated water budget (WB) of the Mediterranean Sea and its various
485 components (E-P-R-B, where R is the river runoff and B the net freshwater flux coming from
486 the Black Sea) shows that, in agreement with the observations, the Mediterranean Sea is an
487 evaporative basin, with a net loss of water through the surface, compensated by a net water
488 mass inflow from the Atlantic through the Strait of Gibraltar. Also the values of the simulated
489 water budget appear to be generally consistent with the observational data (~1.7 mm/day,
490 Sanchez-Gomez et al. 2011). Figure 6 shows the evolution of the simulated WB of the
491 Mediterranean basin for all of the CIRCE integrations. In the second half of the 20th Century,
492 the simulated WB is characterized by some large variability, but no clear long-term trends. In
493 the second part of the integration period (2000-2050), on the other hand, all of the models
494 exhibit a WB significant positive trend, with an ensemble mean value of approximately
495 0.07 ± 0.02 mm/day per decade. The WB increase for the projected period 2021-2050
496 compared to the 1961-1990 mean ranges between 0.15 mm/day (for the ENEA model) and
497 0.35 mm/day (for the CMCC model). In all of the simulations, these changes are mostly due
498 to the decrease found in P, R and B and the increase in E. Specifically, the model projections
499 suggest that the increase in sea-surface evaporation might be as large as +3% (close to the
500 +2.9% found in Mariotti et al. 2008), whereas the reduction in rainfall is of about -9% (larger
501 than the -7.8% found in Mariotti et al. 2008). Therefore, according to the CIRCE projections
502 in the next decades the Mediterranean Sea might loose more water through its surface than in
503 the recent past. Also in this case the CIRCE simulations appear to be in overall agreement

504 with observations and the modelled tendencies are consistent in sign with those observed in
505 the 1960-2000 period (Mariotti et al. 2008).

506 **Changes in the Mediterranean Heat Budget**

507 An analysis of the Mediterranean Sea surface heat budget ($HB=SW+LW+LH+SH$, where
508 SW is the net surface short wave radiation, LW is the net surface long-wave radiation, LH is
509 the latent heat flux and SH is the sensible heat flux) shows that, for all of the CIRCE models,
510 the net budget is negative at the Mediterranean Sea surface, meaning that there is a net heat
511 loss from the sea surface. The simulated HB for the reference period ranges between -1.7
512 W/m^2 (ENEA model) and $-6.4 W/m^2$ (LMD model), whereas the ensemble-mean is of -3.8
513 W/m^2 . These values compare well with the observations (e.g., $-7.0 W/m^2$ from Pettenuzzo et
514 al. 2010 and -3.0 from Sanchez-Gomez et al. 2011), though individually the components of
515 the model HB can differ from the observed ones. Noteworthy, the fact that all of the CIRCE
516 models produce a negative heat budget in the Mediterranean basin and in reasonably good
517 agreement with the observations is an important result. This feature, which is a well-known
518 characteristic of the Mediterranean Sea, in fact, is generally not reproduced by atmospheric
519 only regional models (e.g., Sanchez-Gomez et al. 2011).

520 The simulated negative heat loss at the surface of the Mediterranean is compensated by a
521 gain of heat from the Atlantic through the Strait of Gibraltar. During the control period, all of
522 the CIRCE models show a net positive heat flux entering, through Gibraltar, into the
523 Mediterranean Sea. The simulated values range between 2.3 and $6.3 W/m^2$, well consistent
524 with the estimates obtained from the observations (Sanchez-Gomez 2011 and Pettenuzzo et
525 al. 2010).

526 The projected response for the next decades shows, in all of the models, an increase in SW
527 heat gain (reduced cloud cover), a decrease in the LW heat loss (the increased incoming LW
528 radiation due to the atmospheric greenhouse effect prevails on the increased outgoing LW

529 radiation due to the higher SSTs), a decrease in the SH loss (the air-sea temperature gradient
530 decreases as the atmosphere warms faster than the ocean) and an increase in the LH heat loss
531 (increased evaporation). In all of the CIRCE simulations, the surface net heat loss decreases
532 during the 21st century projections and the projected response in the different heat flux
533 components appear to be consistent among all models. The mean simulated HB for the period
534 2021-2050 is of about -0.8 W/m^2 , leading to a weaker cooling of the ocean by the
535 atmosphere.

536 An extensive analysis of the Mediterranean water budget and heat budget as simulated by
537 the CIRCE models, including a detailed comparison with the observations and a discussion of
538 the projected changes is provided in Dubois et al. (2012).

539 **Changes in the Mediterranean Sea-Level**

540 The CIRCE projections provide also an estimate of the possible sea-level change in the
541 Mediterranean Sea due to the steric effect, which for this basin has been shown to be quite
542 substantial (Marcos and Tsimplis 2008). Combining tide-gauge observations and satellite
543 products, Calafat et al (2009) suggest that the steric effect in the Mediterranean Sea might
544 produce a trend of sea-level change of 0.3 cm/yr for the 1993-2000 period and 0.1 cm/yr for
545 the 1961-2000 time interval. Figure 7 shows the evolution of the simulated steric sea-level
546 change in the CIRCE integrations from 1951 to 2050. During the reference period (1961-
547 1990), the ensemble mean tendency is of $-0.07 \pm 0.2 \text{ cm/yr}$. The models produce a rather broad
548 range of trends, varying from the positive values of the ENEA and CNRM models ($+0.16$ and
549 $+0.17 \text{ cm/yr}$, respectively) to the relatively small negative values of the CMCC and MPI
550 simulations (-0.16 and -0.13 cm/yr , respectively) to the large negative value found for the
551 LMD case (-0.57 cm/yr). The large negative steric trend found in the reference period of the
552 LMD simulation, is most likely due to a remarkable negative temperature drift still present in
553 the Mediterranean Sea water during the early decades of the integration. The cooling is

554 particularly pronounced during the 1951-1970 period (e.g., about $-0.03^{\circ}\text{C}/\text{year}$ in the upper
555 1000 m) and it is probably due to an incomplete spin-up of the model.

556 Throughout the projected period, all of the CIRCE models show significant positive trends
557 of the steric sea-level change (0.29 ± 0.13 cm/yr). The 2021-2050 mean steric sea-level rise
558 ranges between +7 cm and +12 cm, with respect to the reference period. Marcos and Tsimplis
559 (2008), using the A1B CMIP3 simulations, found that the steric effect for the Mediterranean
560 Sea at the end of the 21st Century might account for an average sea-level change ranging
561 between -22 and +18 cm. In the CIRCE projections, therefore, the range of sea-level change
562 appears to be significantly reduced compared to the results of Marcos and Tsimplis (2008).
563 However, the relatively small number of models that form the CIRCE ensemble does not
564 allow performing a robust uncertainty assessment. Therefore, with the present results, we
565 cannot attribute the smaller spread to an actual reduction of the uncertainty produced, in turn,
566 by the improved representation of the Mediterranean Sea in the models.

567 Finally, it is noteworthy that the CIRCE range of steric change is consistent also with
568 Tsimplis et al. (2008), where at the end of a 21st Century SRES A2 projection performed with
569 a coupled atmosphere-ocean regional climate model (Somot et al. 2008) the basin-averaged
570 sea-level rise is of about 13 cm.

571 **4. Concluding remarks**

572 The CIRCE project has made substantial efforts to improve the simulations of the climate
573 of the Mediterranean region, with the aim of providing more reliable climate change
574 projections for this area. In particular, we enhanced the representation of the Mediterranean
575 Sea in the climate system by including ocean components permitting mesoscale circulation
576 features in the Mediterranean basin. For the first time, the evolution of some key sea variable
577 (such as, for example, SST, SSS, sea-level, water and heat fluxes) can be obtained at high

578 resolution over the Mediterranean Sea and with a high degree of physical consistency due to
579 coherent air-sea flux modelling by dedicated coupled atmosphere-ocean models.

580 When compared with the CMIP3 simulations, the CIRCE models show some improvement
581 in reproducing the seasonal means of T2m, precipitation and SST. However, the CIRCE
582 simulations, which include high-resolution air-sea coupling in the Mediterranean region, show
583 significant systematic errors in near-surface temperature and precipitation. Such errors are
584 locally larger than those obtained with regional high-resolution atmospheric only models (e.g.
585 the ENSEMBLES models).

586 The CIRCE models provide a reasonably good estimate of the Mediterranean water budget
587 and, especially, of the surface heat budget. In contrast with most of the ENSEMBLES models,
588 the total heat budget in all of the CIRCE simulations is negative for the present period, with
589 values in good agreement with observations, satisfying the heat closure budget controlled by
590 the heat transport through Gibraltar, also consistent with the observational results.

591 The CIRCE projections indicate that remarkable changes in the Mediterranean region
592 climate might occur already in the early few decades of the scenario. A substantial warming
593 (almost 1.5°C in winter and almost 2°C in summer) and a significant decrease of precipitation
594 (about 5%) might affect the region in the 2021-2050 period compared to the reference period
595 (1961-1990), in an A1B emission scenario. However, locally the changes might be even
596 larger. The projected surface net heat loss decreases in the projected period, leading to a
597 weaker cooling of the Mediterranean Sea by the atmosphere. On the other hand, the water
598 budget appears to increase in the next decades, leading the Mediterranean Sea to loose more
599 water through its surface than in the past. Furthermore, according to the CIRCE projections,
600 the climate change might induce a 2021-2050 mean steric sea-level rise that ranges between
601 +7 cm and +12 cm, with respect to the period of reference.

602 The climate change projections obtained from the CIRCE models are overall consistent
603 with the findings obtained in previous scenario simulations, such as PRUDENCE,
604 ENSEMBLES and CMIP3. The agreement leads to think that these findings are robust to
605 substantial changes in the configuration of the climate models used to produce the scenario
606 simulations. The consensus between the CIRCE projections and the previous findings,
607 especially those obtained from PRUDENCE and ENSEMBLES, shows also that, in general
608 terms, the regional air-sea coupling does not impact strongly the response to anthropogenic
609 climate change.

610 The CIRCE results show also a non-negligible spread, which is, most likely due to
611 differences in the models physics and in the experimental set up, such as the use of global and
612 limited area model configurations, the latter integrated with boundary conditions coming from
613 different global simulations. Also, it is likely that the introduction of the air-sea coupling in
614 the CIRCE simulations contributes to the spread of the responses, although a size of five
615 ensemble members does not allow testing it in a statistical sense. An increase in spread,
616 however, does not necessarily imply an increase in uncertainty in the CIRCE simulations with
617 respect to the results obtained with uncoupled models. The use of uncoupled regional models,
618 as, for example in ENSEMBLES or PRUDENCE, introduces an underestimated uncertainty
619 because the models neglect the physical processes associated with the two-way interaction
620 between atmosphere and ocean, which might be important, as shown in Somot et al. (2008)
621 and Artale et al. (2010).

622 Finally, it is important to keep in mind that despite some improvements, the CIRCE
623 models still have large systematic errors. Therefore, to increase the reliability of the climate
624 change projections, further efforts are required to reduce the biases introduced by the regional
625 air-sea coupling.

626 The most evident and pronounced systematic error in the CIRCE simulations is the cold
627 bias that appears to affect the entire region. As it has been discussed in Dubois et al. (2012),
628 this bias might arise from different sources such as too cold Atlantic water entering at
629 Gibraltar and atmospheric air temperature boundary conditions. However, also problems in
630 the model physical parametrizations (e.g., the surface albedo, especially over the
631 Mediterranean Sea) might contribute to the error.

632 The models discussed here can be improved in many ways, either trying to reduce the
633 systematic errors and improving the representation of important processes. As a first step, for
634 example, the parameterisation of the surface albedo over the Mediterranean Sea could be
635 improved by introducing a dependency on the zenith angle. The change in the albedo
636 representation might have an impact of more than 15 W/m² on the net shortwave radiation
637 (Dubois et al. 2012), affecting thus the surface temperature. Also the representation of the
638 fresh water input, both from the river discharge and the Black Sea, should be enhanced,
639 improving further the water balance of the basin. Moreover, in order to provide more accurate
640 estimates of the possible Mediterranean Sea level rise, the local and remote effects of the
641 atmospheric pressure should be included in the ocean model equations.

642 The regional climate simulations performed within CIRCE represent the first attempt to
643 address the possible climate change in the Mediterranean area using a set of coupled
644 numerical models able to represent the basic physical properties of the Mediterranean Sea,
645 with a multi-model approach. They have represented a seminal effort that will be continued
646 and improved in new international programmes and initiatives such as, for example, HyMeX
647 (Hydrological cycle in the Mediterranean Experiment, Drobinski and Ducrocq 2008) and
648 Med-CORDEX (Mediterranean Coordinated Regional Climate Downscaling Experiment,
649 Ruti et al. 2011).

650 **Acknowledgment**

651 This work has been performed with the support of the CIRCE EU-FP6 Integrated Project,
652 under contract no. GOCE-036961. The authors want to thank the three anonymous reviewers
653 for their suggestions and constructive criticisms. This study also contributes to the
654 Hydrological cycle in the Mediterranean Experiment (HyMex).

655

656 **References**

657 Adani, M., S. Dobricic and N. Pinardi, 2011: Quality Assessment of a 1985–2007
658 Mediterranean Sea Reanalysis. *J. Atmos. Oceanic Technol.*, **28**, 569–589.

659 Artale V., S. Calmanti, A. Carillo, A. Dell’Aquila, M. Herrmann, G. Pisacane, P. Ruti, G.
660 Sannino, M.V. Struglia, F. Giorgi, X. Bi, J. Pal, S. Rauscher, 2010: An atmosphere-ocean
661 regional climate model for the Mediterranean area: assessment of a present-climate
662 simulation. *Clim. Dyn.*, **35**, 721–740.

663 Beuvier J., F. Sevault, M. Herrmann, H. Kontoyiannis, W. Ludwig, M. Rixen, E. Stanev,
664 K. Béranger and S. Somot (2010) Modelling the Mediterranean Sea interannual variability
665 over the last 40 years: focus on the EMT, *J. Geophys. Res.*, doi:10.1029/2009JC005850.

666 Christensen J.H., T.R. Carter, M. Rummukainen, G. Amanatidis, 2007: Evaluating the
667 performance and utility of regional climate models: the PRUDENCE project. *Clim. Change*,
668 **81**, 1-6.

669 Calafat F.M., D. Gomis and M. Marcos (2009): Comparison of Mediterranean sea level
670 fields for the period 1961–2000 as given by a data reconstruction and a 3D model. *Global and*
671 *Planetary Change*, **68**, 175–184.

672 Christensen J.H., M. Rummukainen and G. Lenderink, 2009: Formulation of very-high-
673 resolution regional climate model ensembles for Europe. *ENSEMBLES: Climate Change and*
674 *its Impacts: Summary of research and results from the ENSEMBLES project*. van der Linden
675 P., and J.F.B. Mitchell (eds.) Met Office Hadley Centre, FitzRoy Road, Exeter EX1 3PB, UK.
676 160pp.

677 Dell’Aquila A, Calmanti S, Ruti PM, Struglia MV, Pisacane G, Carillo A, Sannino G
678 2011 Impacts of seasonal cycle fluctuations over the Euro-Mediterranean area using a
679 regional ocean-atmosphere coupled model. *Climate Research*, DOI:10.3354/cr01037.

680 Déqué M, D.P. Rowell, D. Luethi, F. Giorgi, J.H. Christensen, B. Rockel, D. Jacob, E.
681 Kjellström, M. Castro and B. van den Hurk, 2007: An intercomparison of regional climate
682 simulations for Europe: assessing uncertainties in model projections. *Climatic Change* **81**, 53-
683 70

684 Dubois C., S. Somot, S. Calmanti A. Carillo, M. Deque, A. Dell'Aquila, A. Elizalde, S.
685 Gualdi, D. Jacob, B. Lheveder, L.Li, P. Oddo, G. Sannino, E. Scoccimarro and F. Sevault,,
686 2012: Future projections of the surface heat and water budgets of the Mediterranean sea in an
687 ensemble of coupled atmosphere-ocean regional climate models. DOI 10.1007/s00382-011-
688 1261-4

689 Elizalde A., D. Sein, U. Mikolajewick, and D. Jacob, 2010: Technical Report:
690 Atmosphere-ocean-hydrology coupled regional climate model. Max Planck Institute for
691 Meteorology. Available at [http://www.remoc-](http://www.remocm.de/fileadmin/user_upload/remo/UBA/pdf/TechnicalReport.pdf)
692 [m.de/fileadmin/user_upload/remo/UBA/pdf/TechnicalReport.pdf](http://www.remocm.de/fileadmin/user_upload/remo/UBA/pdf/TechnicalReport.pdf)

693 Elizalde A, 2011: The Water Cycle in the Mediterranean Region and the Impacts of
694 Climate Change. *Reports on Earth System Science* N. 103. ISSN 1614-1199, Max Planck
695 Institute for Meteorology, pp 128.

696 Gao X.J., J.S. Pal and F. Giorgi, 2006: Projected changes in mean and extreme
697 precipitation over the Mediterranean region from a high resolution double nested RCM
698 simulation, *Geoph. Res. Letters*, **33**, L03706

699 Gibelin A.L. and M. Déqué, 2003: Anthropogenic climate change over the Mediterranean
700 region simulated by a global variable resolution model. *Clim. Dyn.*, **20**, 327-339

701 Giorgetta M.A., G.P. Brasseur, E. Roeckner and J. Marotzke, 2006: Preface to special
702 section on climate models at the Max Planck Institute for Meteorology. *J Clim.*, **19**, 3769-
703 3770.

704 Giorgi F. 2006: Climate change Hot-spots. *Geophys. Res. Lett.*, 33: L08707.

705 Giorgi F. and P. Lionello, 2008: Climate change projections for the Mediterranean region.
706 *Global Plan. Change*, **63**, 90-104.

707 Glecker P. J., K. E. Taylor, and C. Doutriaux (2007), Performance metrics for climate
708 models, *J. Geophys. Res.*, **113**, D06104, doi:10.1029/ 2007JD008972.

709 Gualdi S., and co-authors, 2012: Future Climate Projections. In *Regional Assessment of*
710 *the Climate Change in the Mediterranean*. Eds A. Navarra and L. Tubiana. Springer Verlag in
711 Press.

712 Hagemann S and D. Jacob, 2007: Gradient in the climate change signal of European
713 discharge predicted by a multi-model ensemble. *Clim. Change*, **81**(Supplement 1), 309–327.

714 Held, I. M., and B. J. Soden, 2006: Robust responses of the hydrological cycle to global
715 warming. *J. Climate*, **19**, 5686–5699.

716 Hourdin F., I. Musat, S. Bony, P. Braconnot, F. Codron, J.-L. Dufresne, L. Fairhead, M.-
717 A. le Filiberti, P. Friedlingstein, J.-Y. Grandpeix, G. Krinner, P. LeVan, Z.-X. Li, F. Lott,
718 2006: The LMDZ4 general circulation model: climate performance and sensitivity to
719 parametrized physics with emphasis on tropical convection. *Clim. Dyn.*, **27**, 787-813.

720 Levitus, S., 1982: *Climatological Atlas of the World Ocean*. NOAA Prof. Paper 13, 173
721 pp. and 17 microfiche.

722 Lopez-Moreno, M. Beniston and J.M. Garcia-Ruiz: Environmental change and water
723 management in the Pyrenees: Facts and future perspectives for Mediterranean mountains.
724 *Global Plan. Change*, **61**, 300-312.

725 Ludwig W, Dumont E, Meybeck M. and S. Heussner, 2009: River discharges of water and
726 nutrients to the Mediterranean Sea: major drivers for ecosystem changes during past and
727 future decades? *Prog Oceanogr* **80**, 199–217

728 Marcos M., and M. Tsimplis, 2008: Comparison of results of AOGCMs in the
729 Mediterranean Sea during the 21st century. *J. Geophys. Res.*, **113**,
730 doi:10.1029/2008JC004820.

731 Mariotti, A., and co-authors, 2008: Mediterranean water cycle changes: transition to drier
732 21st century conditions in observations and CMIP3 simulations, *Env Res Lett.*
733 doi:10.1088/1748-9326/3/044001

734 MEDAR-Group: MEDATLAS 2002 Database, Cruise Inventory, observed and analyzed
735 data of temperature and bio-chemical parameters, IFREMER Edition (4 CDRom), 2002.

736 Meehl, G.A., C. Covey, T. Delworth, M. Latif, B. McAvaney, J.F.B. Mitchell, R.J.
737 Stouffer and K.A. Taylor, 2007: The WCRP CMIP3 multimodel dataset - A new era in
738 climate change research. *Bull. Amer. Meteor. Soc.*, **88**, 1383-1394.

739 Mitchell T. D. and P.D. Jones, (2005): An improved method of constructing a database of
740 monthly climate observations and associated high-resolution grids. *Inter. Int. J. Climatol*, **25**,
741 693 – 712.

742 Nakićenović, N., and R. Swart (eds.) (2000): Special Report on Emissions Scenarios. A
743 Special Report of Working Group III of the Intergovernmental Panel on Climate Change.
744 Cambridge University Press, Cambridge, United Kingdom and New York, NY, USA, 599 pp.

745 Oddo P., M. Adani, N. Pinardi, C. Fratianni, M. Tonani, and D. Pettenuzzo, 2009: A
746 nested Atlantic-Mediterranean Sea general circulation model for operational forecasting
747 *Ocean Sci. Discuss.*, **6**, 1093-1127.

748 Oki, T. and Y.C. Sud, 1998: Design of Total Runoff Integrating Pathways (TRIP): A
749 global river channel network. *Earth Int.*, Vol. 2, 53 pp.

750 Pincus R., C.P. Batstone, R.J.P. Hofmann, K. E. Taylor and P.J. Glecker, 2008: Evaluating
751 the present-day simulation of clouds, precipitation, and radiation in climate models. *J.*
752 *Geophys. Res.*, **113**, D14209, doi:10.1029/2007JD009334

753 Rayner, N. A., D. E. Parker, E. B. Horton, C. K. Folland, L. V. Alexander, D. P. Rowell,
754 E. C. Kent, and A. Kaplan, 2003: Global analyses of sea surface temperature, sea ice, and
755 night marine air temperature since the late nineteenth century. *J. Geophys. Res.*, **108**, 4407,
756 doi:10.1029/2002JD002670.

757 Ruti P. and the MEDCordex Community - MED2C Team, 2011: MED-CORDEX
758 initiative for Mediterranean Climate studies. *Geophysical Research Abstracts*, Vol. 13,
759 EGU2011-10715.

760 Sanchez-Gomez E., S. Somot, S.A. Josey, C. Dubois, N. Elguindi, M. Déqué, 2011:
761 Evaluation of the Mediterranean Sea Water and Heat budgets as simulated by an ensemble of
762 high resolution Regional Climate Models. *Clim. Dyn.*, DOI 10.1007/s00382-011-1012-6.

763 Sanchez-Gomez E., S. Somot and A. Mariotti, 2009: Future changes in the Mediterranean
764 water budget projected by an ensemble of Regional Climate Models. *Geophys. Res. Lett.*, **36**,
765 L21401, doi:10.1029/2009GL040120.

766 Sannino, G., M. Herrmann, A. Carillo, V. Rupolo, V. Ruggiero, V. Artale, P. Heimbach-
767 2009a An eddy-permitting model of the Mediterranean Sea with a two-way grid refinement at
768 Gibraltar- Ocean Modelling doi: 10.1016/j.ocemod.2009.06.002.

769 Sannino, G., L. Pratt and A. Carillo, 2009b. Hydraulic Criticality of the Exchange Flow
770 through the Strait of Gibraltar. *J. Phys. Oceanogr.* **39**, 2779–2799.

771 Scoccimarro E, Gualdi S, Bellucci A, Sanna A, Fogli PG, Manzini E, 1549 Vichi M, Oddo
772 P. and A. Navarra, 2011: Effects of tropical cyclones on ocean heat transport in a high-
773 resolution coupled general circulation model. *J Climate* **24**, 4368–4384.

774 Somot S., F. Sevault and M. Déqué, 2006: Transient climate change scenario simulation of
775 the Mediterranean Sea for the 21st century using a high-resolution ocean circulation model.
776 *Clim. Dyn.*, **27**, 851-879.

777 Somot S., F. Sevault, M. Déqué and M. Crépon, 2008: 21st century climate change
778 scenario for the Mediterranean using a coupled Atmosphere-Ocean Regional Climate Model.
779 *Global and Planetary Change*, **63**, 112-126.

780 Taylor, K. E. (2001), Summarizing multiple aspects of model performance in a single
781 diagram, *J. Geophys. Res.*, **106**(D7), 7183– 7192.

782 Thorpe, R., and G. Bigg, 2000: Modelling the sensitivity of the mediterranean outflow to
783 anthropogenically forced climate change, *Clim. Dyn.*, **16**, 355–368.

784 Tsimplis M., Marcos M., Somot S. (2008) 21st century Mediterranean sea level rise: steric
785 and atmospheric pressure contributions from a regional model. *Global and Planetary Change*,
786 **63**(2-3): 105-111, doi:10.1016/j.gloplacha.2007.09.006

787 Ulbrich U., and co-authors, 2012: Past and current climate changes in the Mediterranean
788 Region. In *Regional Assessment of the Climate Change in the Mediterranean*. Eds A. Navarra
789 and L. Tubiana. Springer Verlag in Press.

790 Valcke, S., 2006: OASIS3 User Guide (prism_2-5). CERFACS Technical Report
791 TR/CMGC/06/73, PRISM Report No 3, Toulouse, France. 60 pp.

792 Van Leer B., 1979: Towards the ultimate conservative difference scheme, V. A Second
793 Order Sequel to Godunov's Method. *J. Com. Phys.*, **32**, 101–136.

794 Zou L., Z. Tianjun, L. Li and Z. Jie, 2010: East china summer rainfall variability of 1958–
795 2000: dynamical downscaling with a variable-resolution AGCM. *J. Climate*, **23**, 6394–6408.

Model	Atmosphere component	Global Ocean component	Mediterranean Sea component	Gibraltar and Lateral Boundary Conditions	Rivers and Black sea
CMCC (INGV) (Scoccimarro et al. 2011)	ECHAM5 80km, L31	OPA8.2 - ORCA2 grid ~ 2°x2° (0.5° equator), L31	NEMO-MFS 1/16° (~ 7km), L71 (Oddo et al. 2009)	Fluxes exchanged between global ocean and Mediterranean Sea. Mediterranean outflow distributed over the upper 300m in the global ocean grid point near Gibraltar.	TRIP river scheme (Nile runoff corrected to the observations after 1968). Black sea input from the E-P-R flux (Oki and Sud, 1998).
LMD (IPSL) (Hourdin et al. 2006, Zou et al. 2010)	LMDZ global + LMDZ regional 300 km, L19 + 30 km, L19	OPA9 - ORCA2 ~ 2°x2° (0.5° equator), L31	NEMO-MED8 1/8° (9-12 km), L43 (Beuvier et al. 2010)	Tracer profile and fluxes exchanged using Cross-Land Advection parameterisation and buffer zone .	Climatological river discharge (Ludwig et al. 2009).
CNRM (Météo France/ CNRM) (Somot et al., 2008)	ARPEGE-Climate TL159c2.5 , stretched model: 50x50 km over Euro-Mediterranean-North Africa) L31	OPA9 - ORCA2 ~ 2°x2° (0.5° equator), L31	NEMO-MED8 1/8° (9-12 km), L43 (Beuvier et al. 2010)	Tracer profile and fluxes exchanged using Cross-Land Advection parameterisation and buffer zone.	Climatological river discharge (Ludwig et al. 2009).
PROTHEUS (ENEA) (Artale et al., 2010)	REG-CM3 30 km, L19	-	MIT-gcm 1/8° (9-12 km), L42 (Sammino et al. 2009a)	Atlantic buffer zone. Lateral Boundaries from ECHAM5/MPI-OM (Giorgetta et al. 2006).	IRIS rivers scheme. Instantaneous runoff to the river mouth. Black sea input from E-P-R budget bias corrected.
MPI (MPI-HH) (Elizalde 2011)	REMO 25 km, L31	-	MPI-OM 9 km, L29 (Elizalde et al. 2010)	Atlantic buffer zone. Lateral Boundaries from CMCC. (Scoccimarro et al, 2011).	Interactive hydrological model and Black sea model (Hagemann and Jacob 2007).

797

798 **Table 1:** summary of the basic features of the CIRCE models and their implementation. References indicate where a more detailed description of
799 the models, their features and performances are described and discussed.

Acronym	CMIP3 model name	Centre	Atmospheric resolution	Oceanic resolution
BCCR	BCCR-BCM2.0	Bjerknes Centre for Climate Research (Norway)	2.81° x 2.81° L31	1.5°x(1.5° - 0.5°) L35
CNRM	CNRM-CM3	Météo-France / Centre National de Recherches Météorologiques (France)	2.81° x 2.81° L45	2°x(1.5° - 0.5°) L31
CSIRO	CSIRO-Mk3.5	CSIRO Atmospheric Research (Australia)	1.88° x 1.88° L18	1.88° x 0.84° L31
GFDL	GFDL-CM2.1	US Dept. of Commerce / NOAA / Geophysical Fluid Dynamics Laboratory (USA)	2.5° x 2° L24	1°x(1° - 0.33°) L50
IAP	FGOALS-g1.0	LASG / Institute of Atmospheric Physics (China)	2.81° x 2.81° L26	1°x(1° - 0.33°) L30
IPSL	IPSL-CM4	Institut Pierre Simon Laplace (France)	3.75° x 2.5° L19	2°x(1.5° - 0.5°) L31
MIROC	MIROC3.2(hires),	CCSR/NIES/FRCGC (Japan)	1.1° x 1.1° L56	0.28° x 0.19° L47
MPI	ECHAM5/MPI-OM	Max Planck Institute for Meteorology (Germany)	1.88° x 1.88° L31	1.5° x 1.5° L40
NCAR	CCSM3	National Center for Atmospheric Research (USA)	1.4° x 1.4° L26	1°x(1.1° - 0.27°) L40
UKMO	HADCM3	Hadley Centre for Climate Prediction and Research / Met Office (UK)	3.75° x 2.5° L38	1.25° x 1.25°

801

802 **Table 2:** List of models and relative resolution (atmosphere and ocean). The grid interval is approximate, as it
803 may vary across latitudes and may be different in the longitude and latitude directions. The reader is referred to
804 the PCMDI web site [http:// www.pcmdi.llnl.gov](http://www.pcmdi.llnl.gov) for more information on models and experiments.

805

806

FIGURE CAPTIONS

807 **Figure 1:** orography of the Euro-Mediterranean region and bathymetry of the Mediterranean
808 Sea as represented in a state-of-the-art global coupled ocean-atmosphere model with
809 horizontal resolution of about 300 Km in the atmosphere and 1° in the ocean (panels a and b),
810 and in the CIRCE models where in most of the models the resolution is higher than 50 Km in
811 the atmosphere and 1/8° in the ocean.

812

813 **Figure 2:** scheme of the basic characteristics of the CIRCE models. Left: set up of the models
814 with a high-resolution Mediterranean Sea component coupled with a global ocean and a
815 global atmosphere (INGV, IPSL and METEOFrance models). Right: set up of the models
816 where the high-resolution Mediterranean Sea component is coupled with a high-resolution
817 limited area atmospheric model (ENEA and MPI models).

818

819 **Figure 3:** Taylor diagrams of SST (panel a, DJF mean, panel b JJA mean), T2m over land
820 (panel c, DJF mean, panel d JJA mean) and precipitation over land (panel e, DJF mean, panel
821 f JJA mean). The plot summarizes the pattern correlation, root mean square difference, and
822 spatial standard deviation of each of the CMIP3 and CIRCE models with respect to
823 observations (SST Mediterranean re-analysis, Adani et al. 2011 and CRU TS 3, Mitchell and
824 Jones, 2005) over the Mediterranean area (28°-48°N, 9.5°W-38.5°E).

825

826 **Figure 4:** evolution of the sea-surface temperature (SST) anomalies from 1951 to 2050 as
827 simulated with the CIRCE models (thin black lines) and with the CMIP3 models (red dashed
828 line). The anomalies are expressed in °C and have been computed with respect to the 1961-
829 1990 mean. The thick, black curve is the CIRCE multi-model mean, whereas the shading is
830 the CIRCE multi-model standard deviation with respect to the multi-model mean. In order to

831 highlight the long-term trends, the interannual variability has been filtered by applying 5-year
832 running mean.

833

834 **Figure 5:** change in seasonal mean 2-meter land temperature (T2m, left panels) and mean
835 precipitation (right panels) obtained from the CIRCE and the CMIP3 simulations for the
836 2021-2050 period compared to the reference (1961-1990) period. The CIRCE models are
837 indicated with the + symbol, whereas the filled black circles represent the CIRCE multimodel
838 ensemble means and the filled red squares represent the CMIP3 multimodel ensemble means.
839 Upper panels show the changes for the winter (DJF); lower panels show the changes for the
840 summer (JJA). The differences have been computed for seven areas of the Mediterranean
841 region defined according to Giorgi and Lionello (2008). Units are °C for T2m and % of the
842 reference period value for precipitation.

843

844 **Figure 6:** as in Figure 3, but for the water budget of the Mediterranean basin expressed in
845 mm/day. The budget is computed as the difference between Evaporation, Precipitation and
846 Runoff averaged over the Mediterranean Sea and the contribution from the Black Sea (E-P-R-
847 B).

848

849 **Figure 7:** as in Figure 4, but for the steric component of the sea level change. The plotted
850 values (cm) show the evolution of the simulated sea-level change due to the steric effect.
851 Steric anomalies are computed with respect to the reference period (1961-1990).

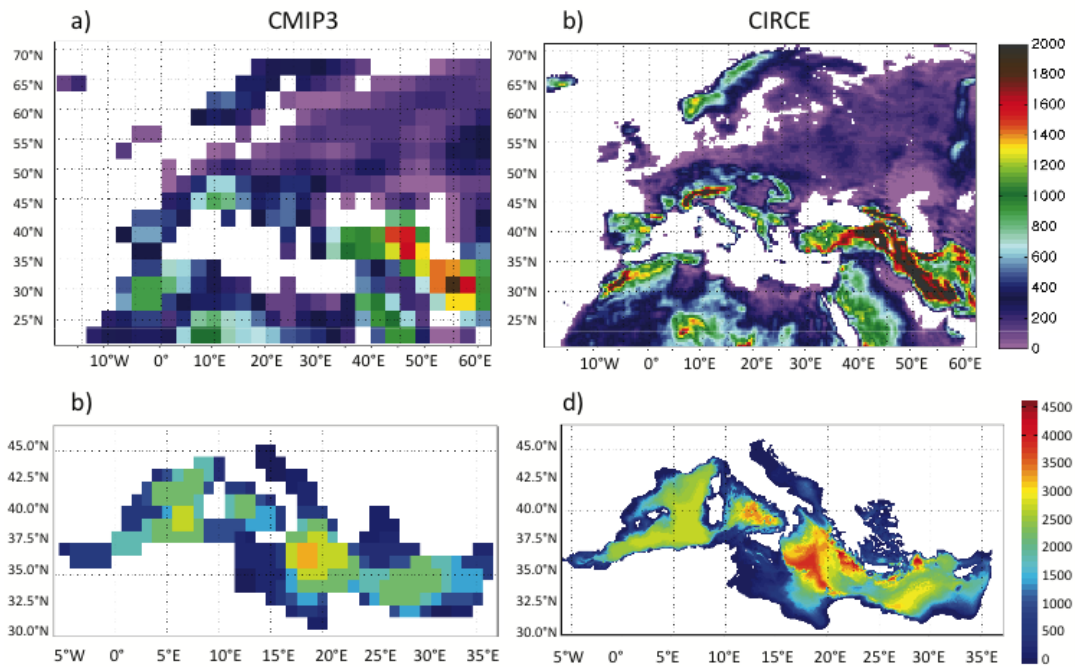
852

853

854

FIGURES

855



856

857 **Figure 1:** orography of the Euro-Mediterranean region and bathymetry of the Mediterranean

858 Sea as represented in a state-of-the-art global coupled ocean-atmosphere model with

859 horizontal resolution of about 300 Km in the atmosphere and 1° in the ocean (left column

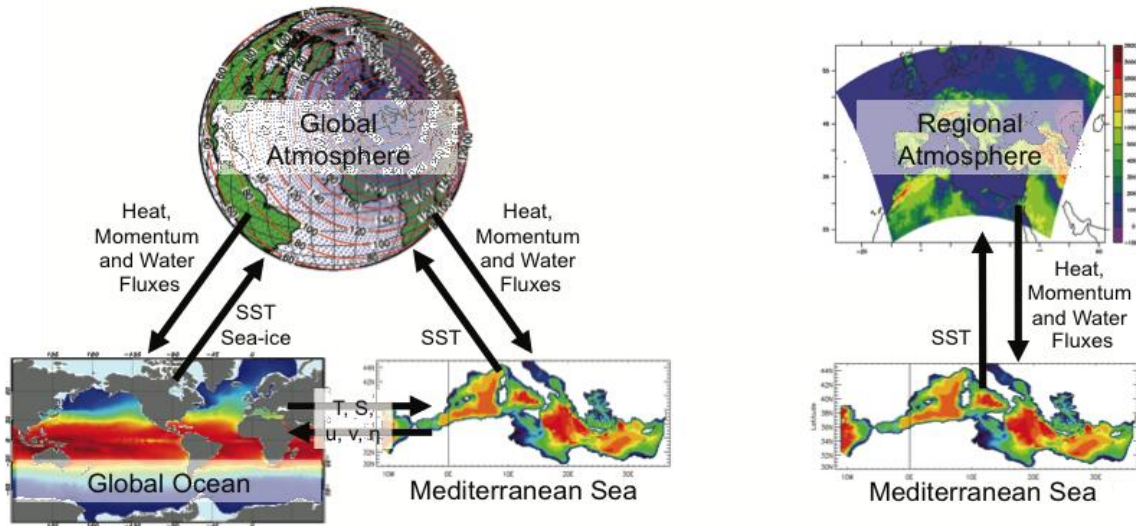
860 panels, a and b), and in the CIRCE models where in most of the models the resolution is

861 higher than 50 Km in the atmosphere and 1/8° in the ocean (right column panels, c and d).

862

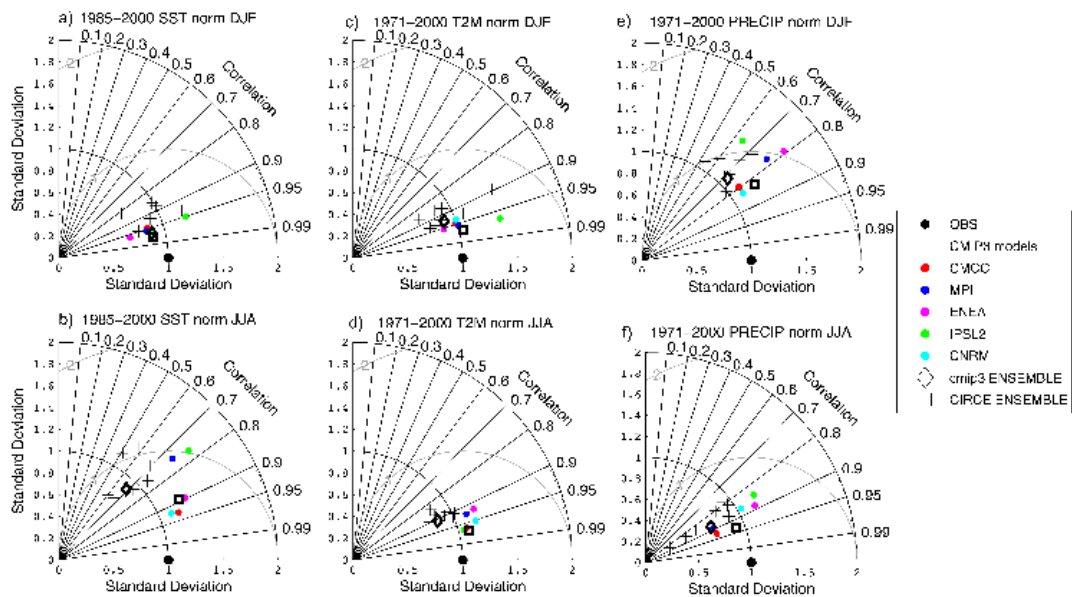
863

864
865
866



867
868
869
870
871
872
873
874

Figure 2: scheme of the basic characteristics of the CIRCE models. Left: set up of the models with a high-resolution Mediterranean Sea component coupled with a global ocean and a global atmosphere (INGV, LMD and CNRM models). Right: set up of the models where the high-resolution Mediterranean Sea component is coupled with a high-resolution limited area atmospheric model (ENEA and MPI models).



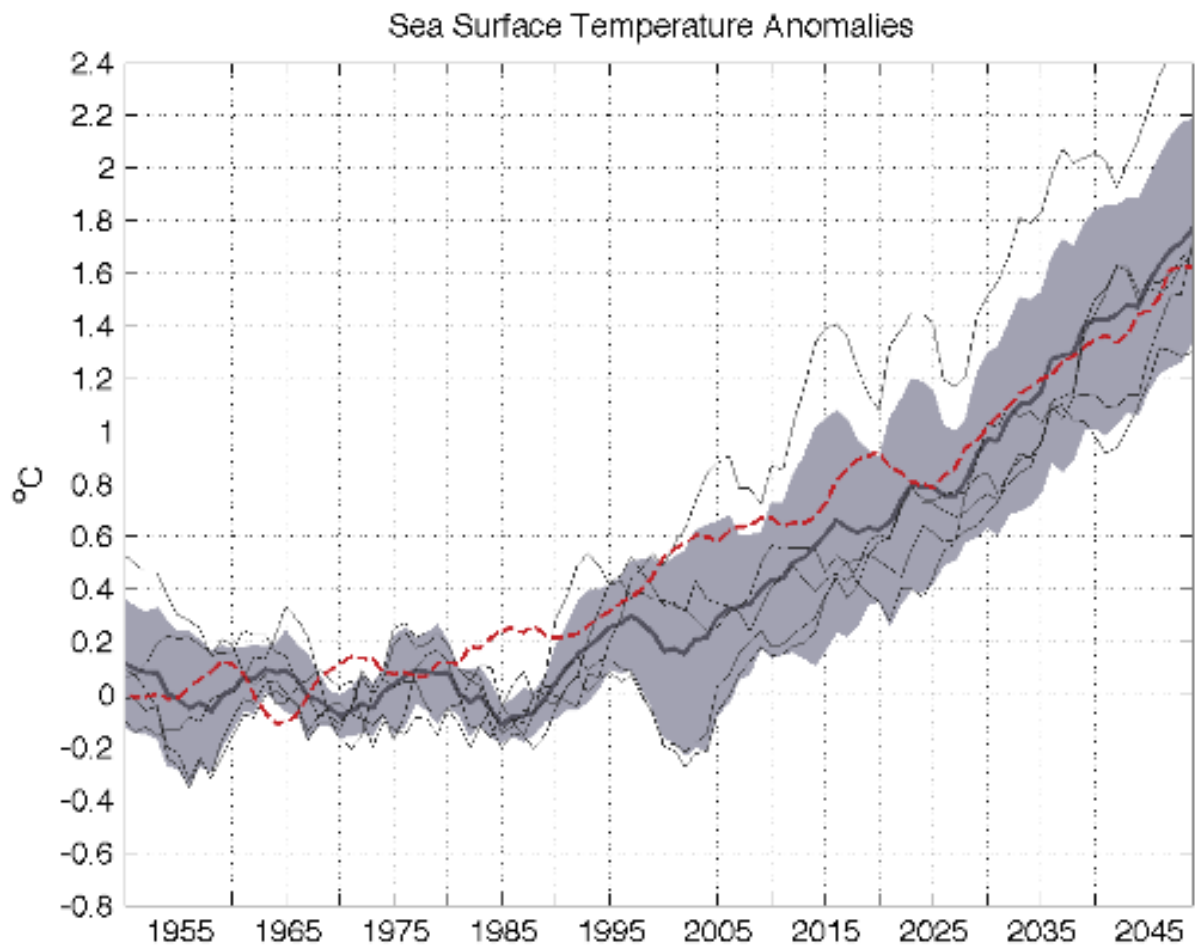
876

877 **Figure 3:** Taylor diagrams of SST (panel a, DJF mean, panel b JJA mean), T2m over land
 878 (panel c, DJF mean, panel d JJA mean) and precipitation over land (panel e, DJF mean, panel
 879 f JJA mean). The plot summarizes the pattern correlation, root mean square difference, and
 880 spatial standard deviation of each of the CMIP3 and CIRCE models with respect to
 881 observations (SST Mediterranean re-analysis, Adani et al. 2011 and CRU TS 3, Mitchell and
 882 Jones, 2005) over the Mediterranean area (28° - 48° N, 9.5° W- 38.5° E).

883

884

885



886

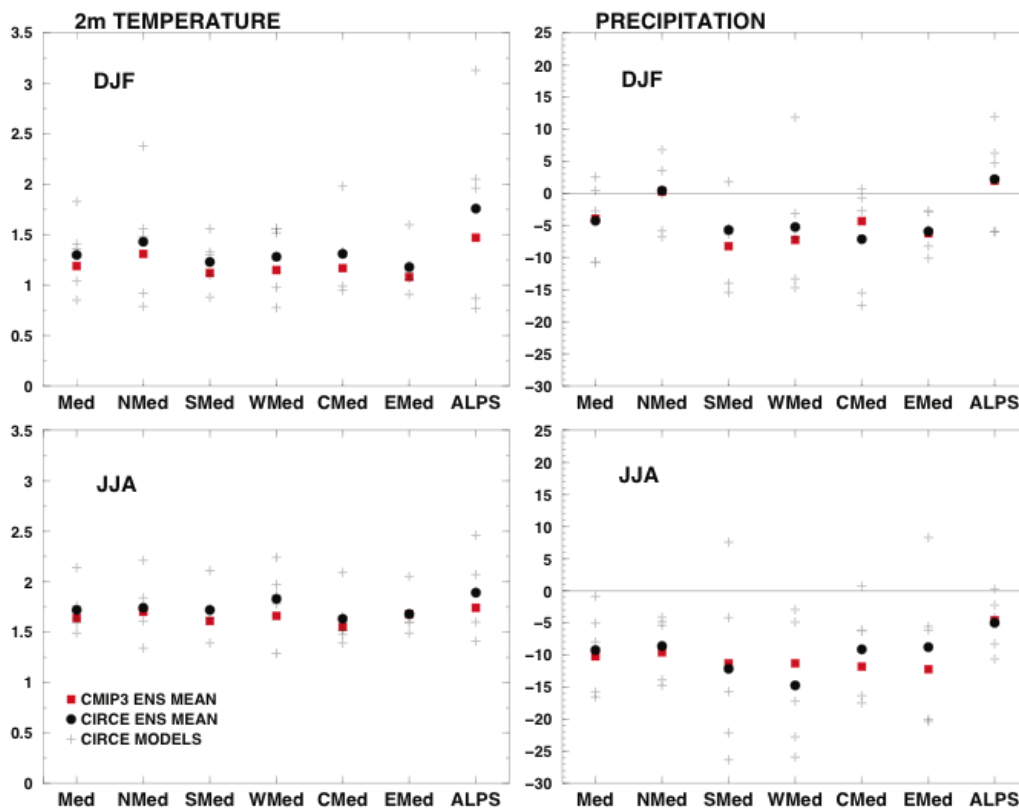
887 **Figure 4:** evolution of the sea-surface temperature (SST) anomalies from 1951 to 2050 as
888 simulated with the CIRCE models (thin black lines) and with the CMIP3 models (red dashed
889 line). The anomalies are expressed in °C and have been computed with respect to the 1961-
890 1990 mean. The thick, black curve is the CIRCE multi-model mean, whereas the shading is
891 the CIRCE multi-model standard deviation with respect to the multi-model mean. In order to
892 highlight the long-term trends, the interannual variability has been filtered by applying 5-year
893 running mean.

894

895

896

897



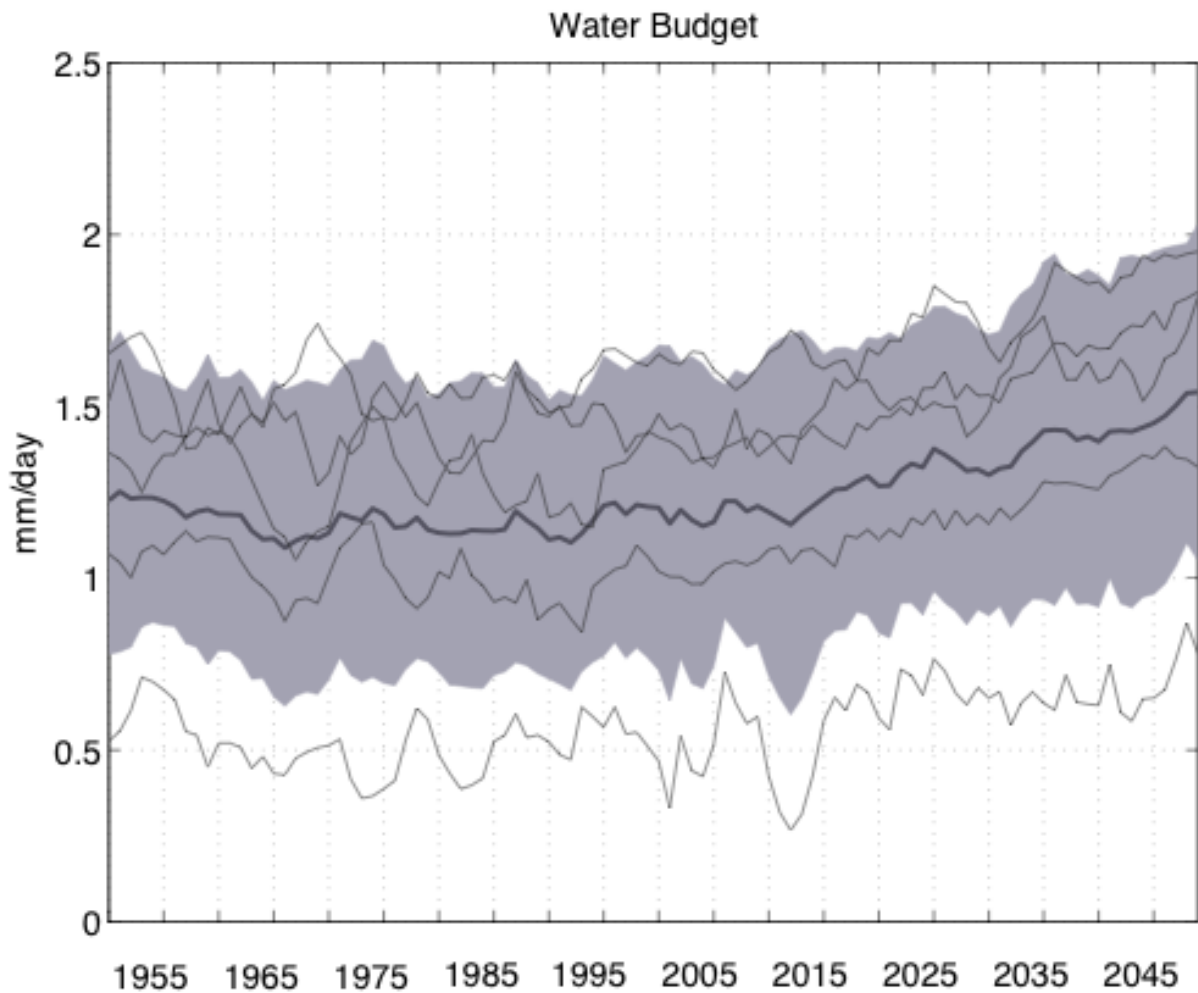
898

899 **Figure 5:** change in seasonal mean 2-meter land temperature (T2m, left panels) and mean
900 precipitation (left panels) obtained from the CIRCE and the CMIP3 simulations for the 2021-
901 2050 period compared to the reference (1961-1990) period. The CIRCE models are indicated
902 with the + symbol, whereas the filled black circles represent the CIRCE multimodel ensemble
903 means and the filled red squares represent the CMIP3 multimodel ensemble means. Upper
904 panels show the changes for the winter (DJF); lower panels show the changes for the summer
905 (JJA). The differences have been computed for seven areas of the Mediterranean region
906 defined according to Giorgi and Lionello (2008). Units are °C for T2m and % of the reference
907 period value for precipitation.

908

909

910
911
912



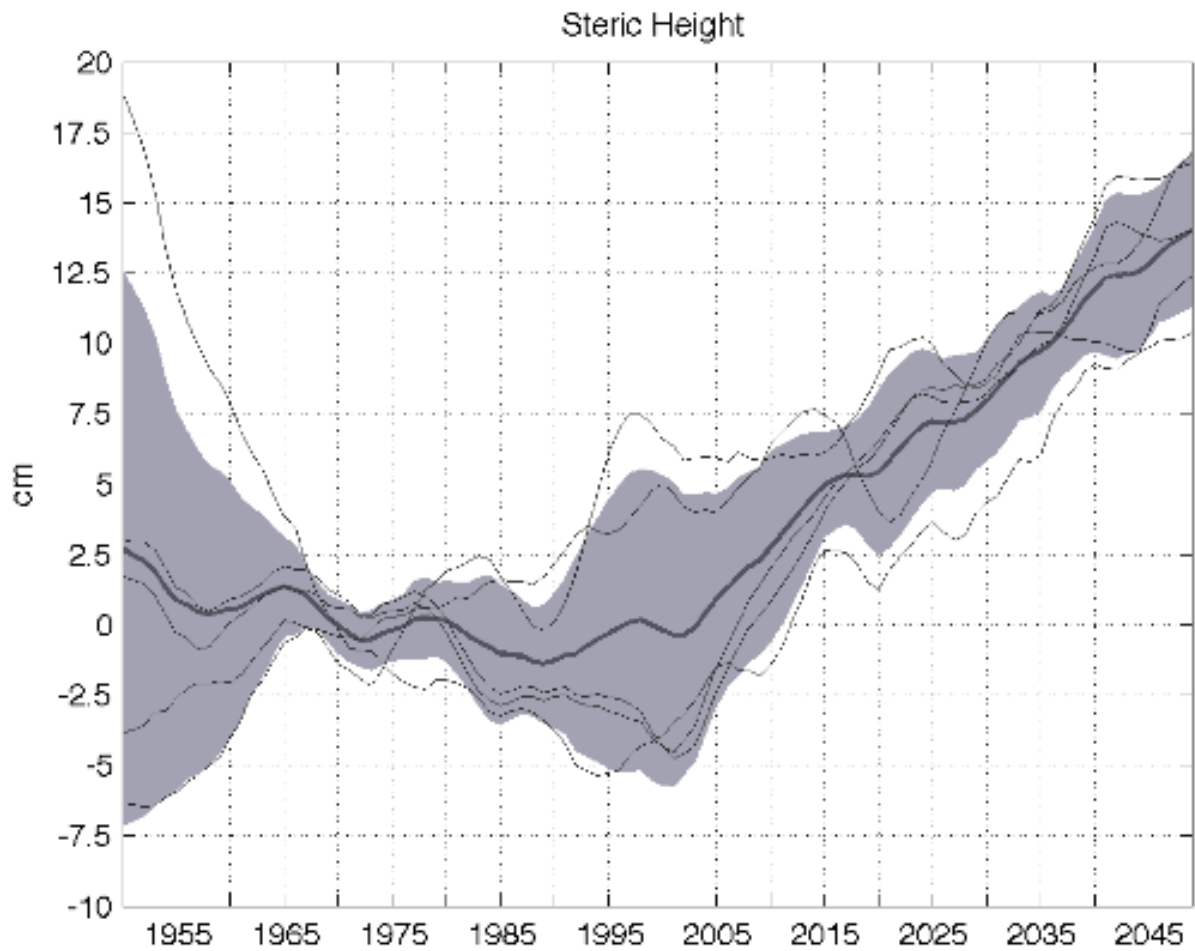
913
914
915
916
917
918

Figure 6: as in Figure 4, but for the water budget of the Mediterranean basin expressed in mm/day. The budget is computed as the difference between Evaporation, Precipitation and Runoff averaged over the Mediterranean Sea and the contribution from the Black Sea (E-P-R-B).

919

920

921

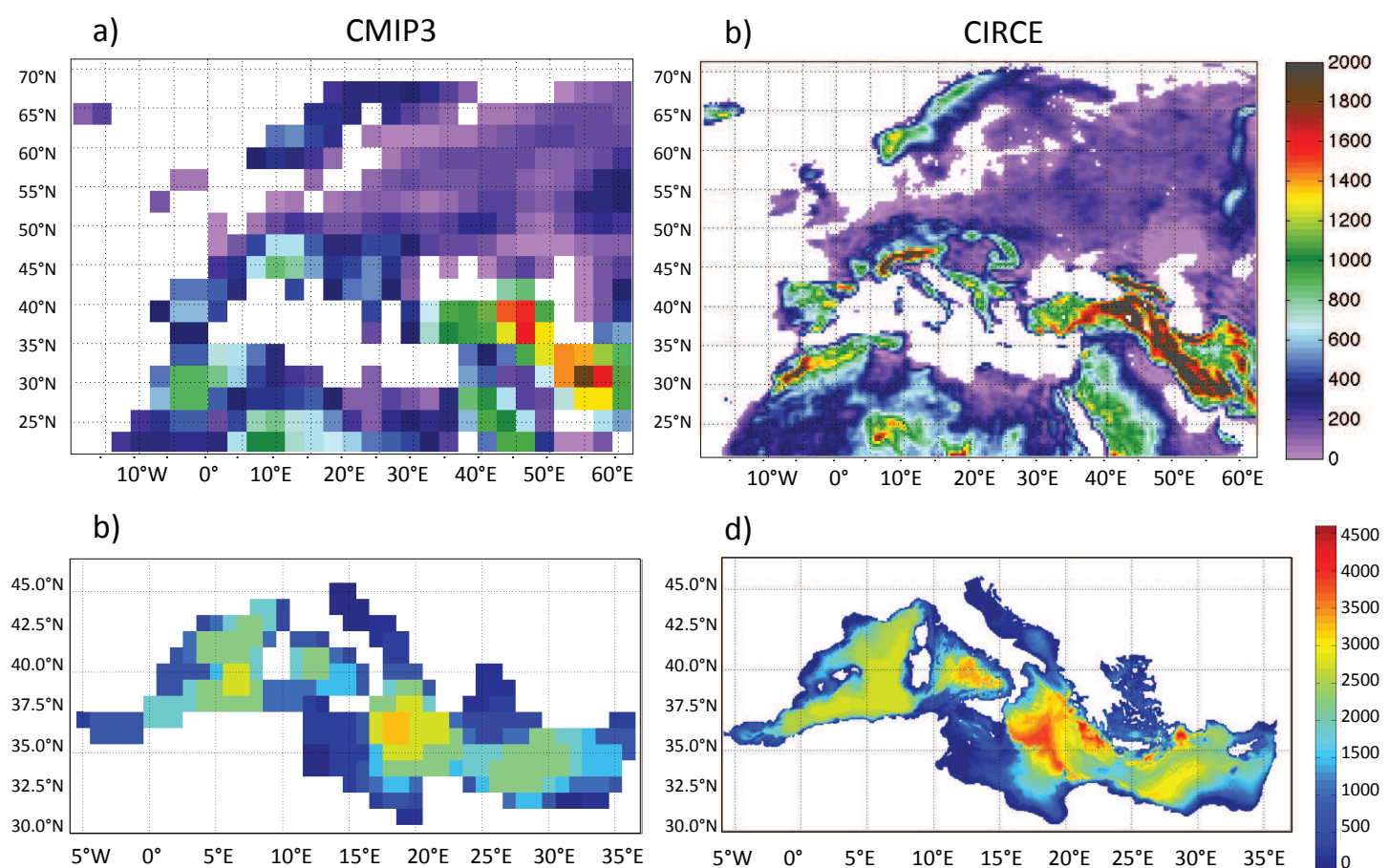


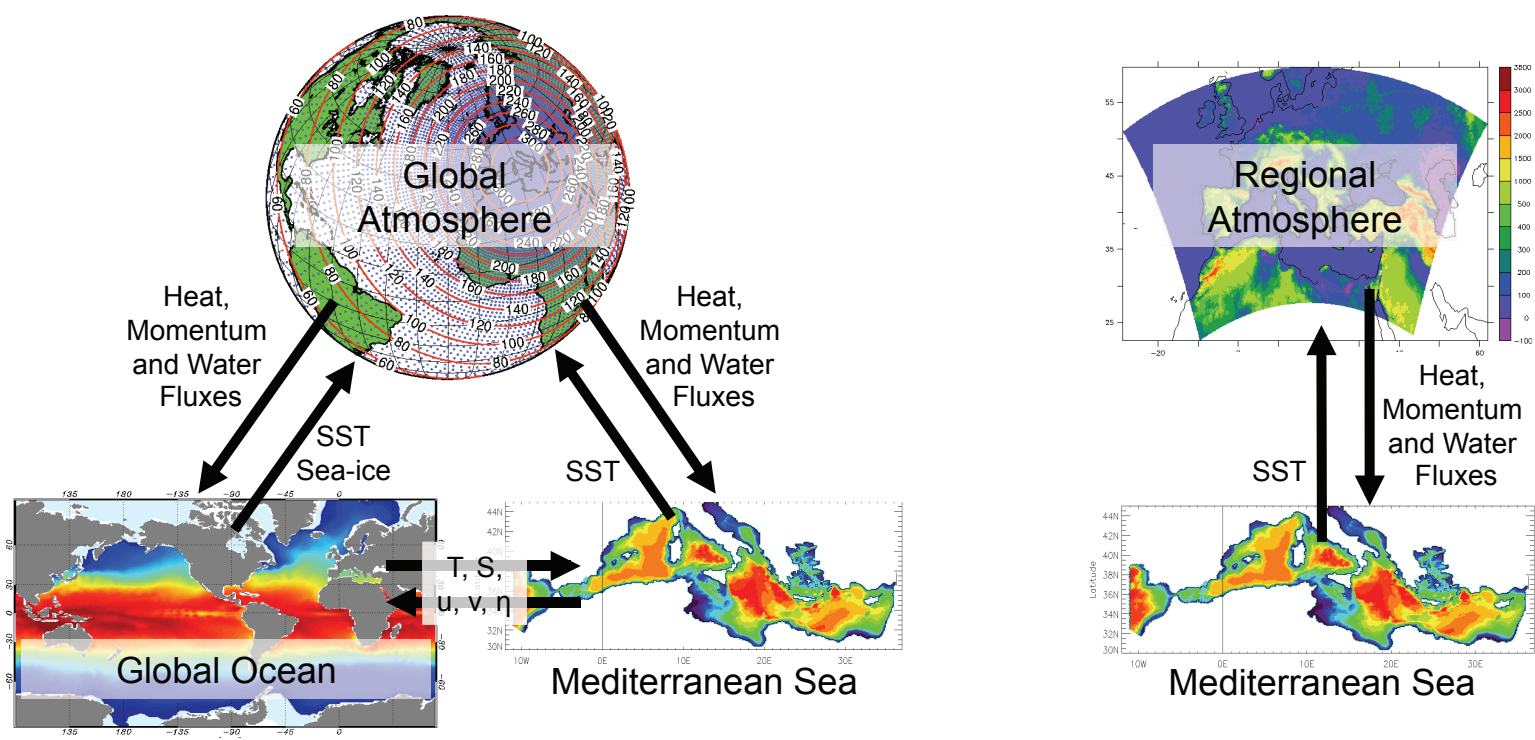
922

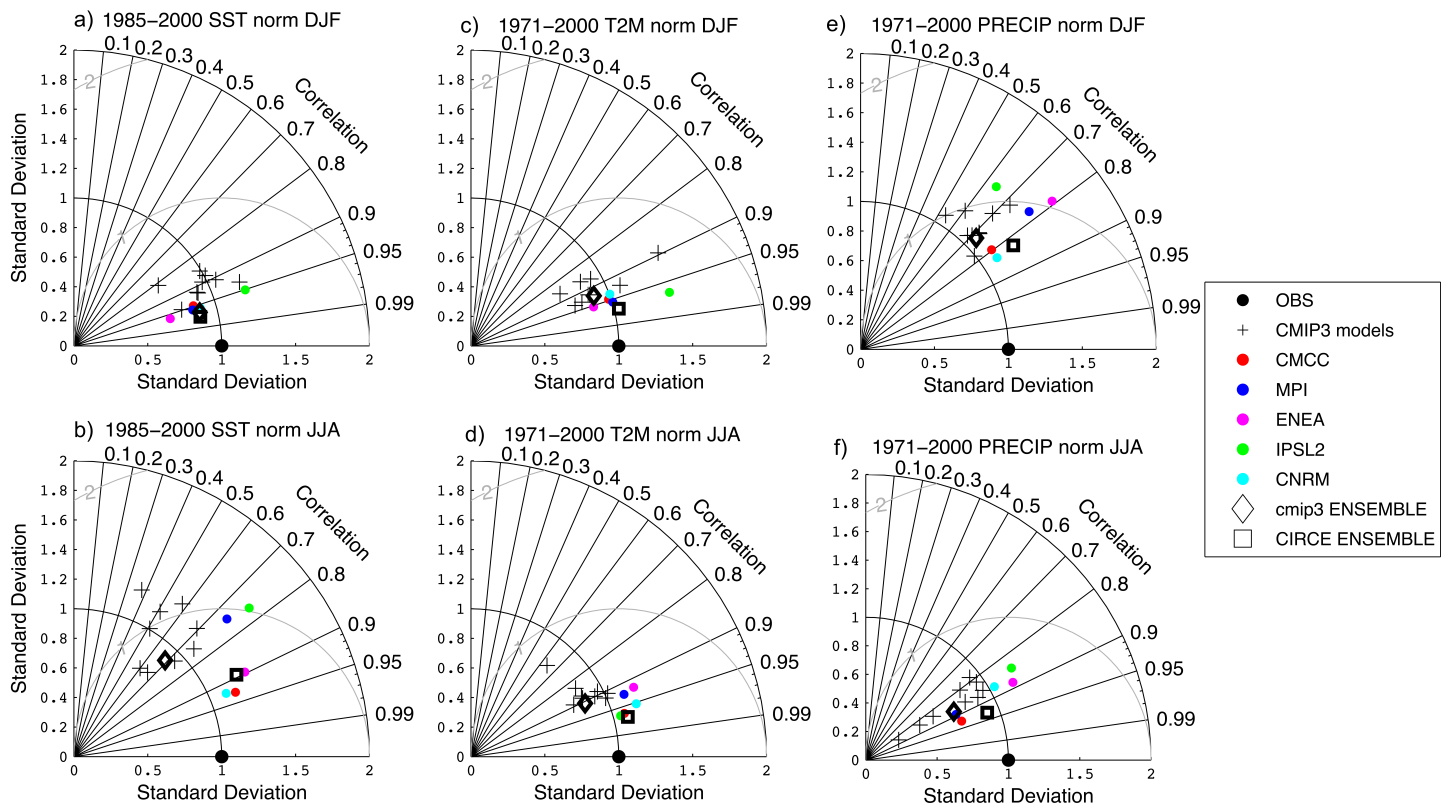
923 **Figure 7:** as in Figure 4, but for the steric component of the sea level change. The plotted

924 values (cm) show the evolution of the simulated sea-level change due to the steric effect.

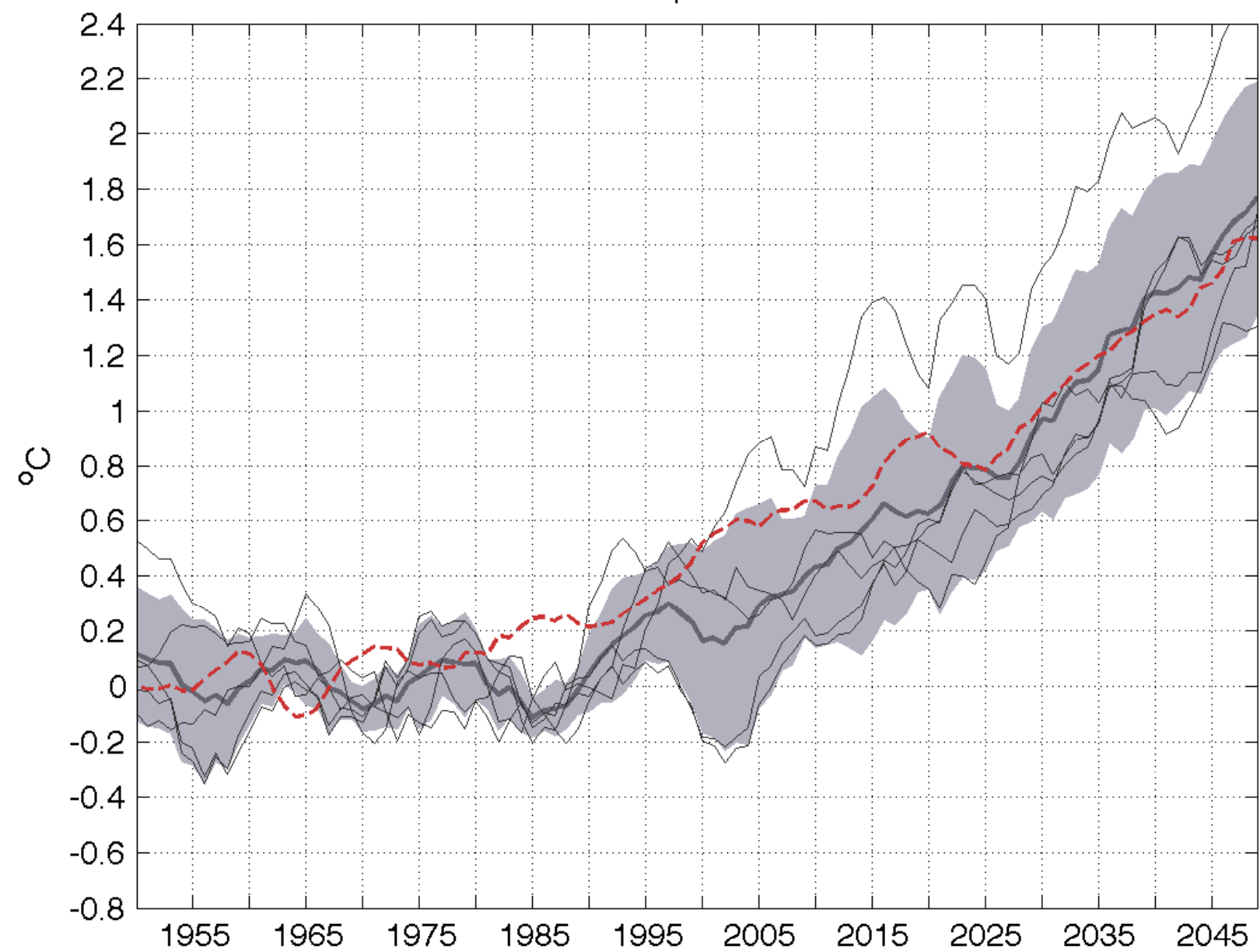
925 Steric anomalies are computed with respect to the reference period (1961-1990).

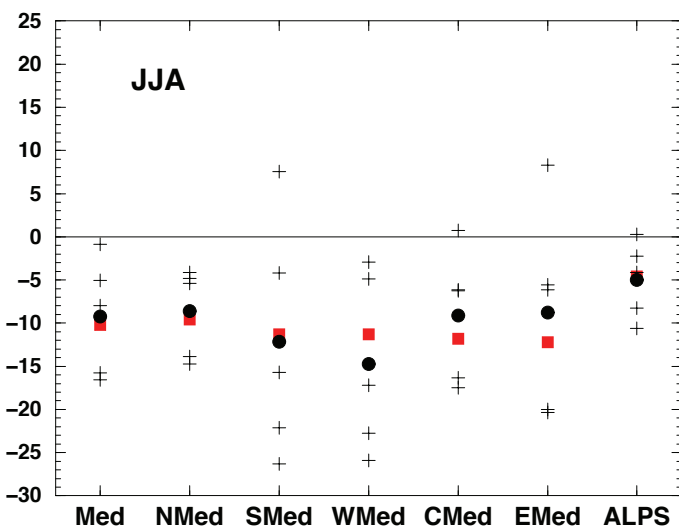
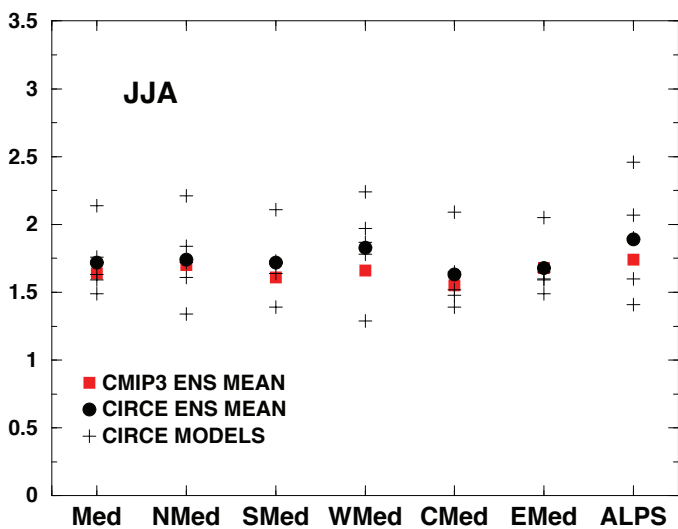
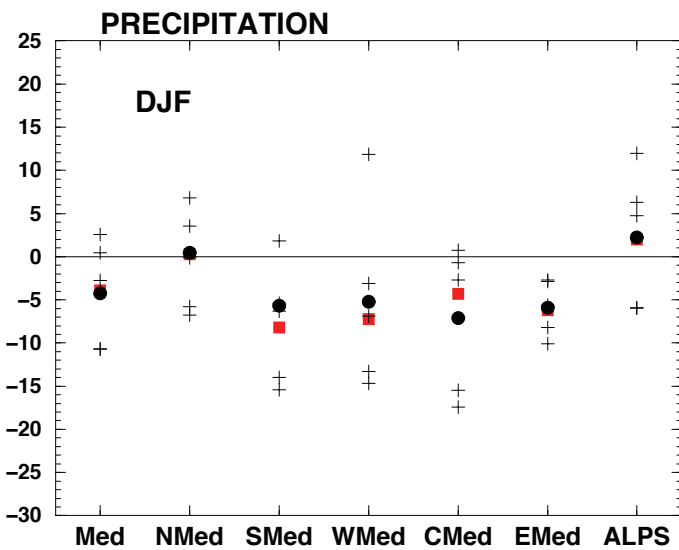
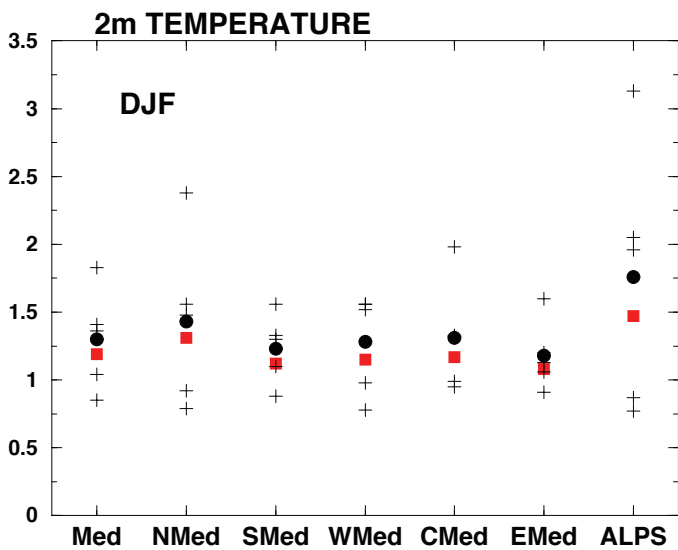






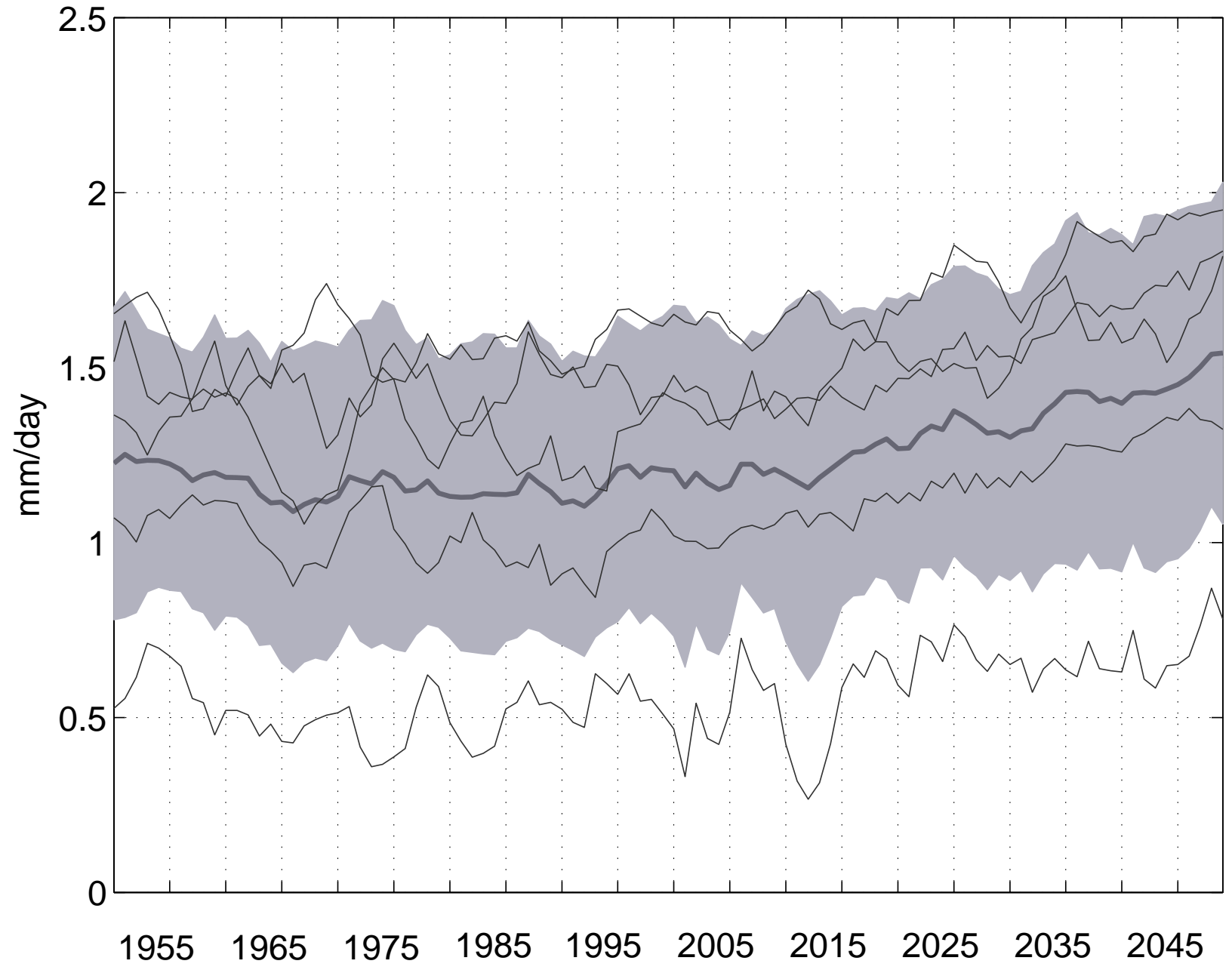
Sea Surface Temperature Anomalies





■ CMIP3 ENS MEAN
● CIRCE ENS MEAN
+ CIRCE MODELS

Water Budget



Steric Height

